Chapter 5 Cobalt-rich Crusts

5 - 1 Classification and Layered Structure of Cobalt-rich Crusts

(1) Classification of cobalt-rich crusts

The collected samples accompanied by cobalt-rich crusts are classified into the following three types; namely crusts, cobble crusts, and nodules. When the average thickness of the cobalt-rich crust is less than 1mm, they are classified as rock samples, and the term "coating" is used when the crust covers the whole sample and "stain" is used when the crust is merely attached locally. Also when the host rock is not confirmed, it is described as crust fragment.

Photographs of typical crusts are shown in Figure 5-1-1(1)(2).

1) Crusts

Crusts are material whose upper surfaces and the sides are covered by cobalt-rich crusts and fresh substrates are exposed on the bottom surfaces. The substrates are mostly rocks, but in rare cases they are consolidated clay.

The crusts are often separated from the substrates during sampling, and collected as crust fragments without substrates. These crusts are classified as "crusts" in calculating the amount of samples collected and for other statistical purposes, but are separated from those with substrates as crusts "fragments" in description of each sample.

2) Cobble crusts

Cobble crusts are cobble-shaped material exceeding 8cm in long axis, and whose entire surface is covered by cobalt-rich crust. Those with only coating or stains on the sides and bottom are also classified as cobble crusts.

Many nuclei are; lava fragments, fragmented rocks, rocks torn from the basement such as talus and floats, but some are crust fragments separated from the slopes and nodules. The crust is generally developed on the upper surface, and, as a rule, the surface with thick crust is defined as the upper surface in this survey.

3) Nodules

Nodules are material smaller than 8cm in diameter and are covered entirely by cobalt-rich crust. Nodules, similar to cobble crusts, have nuclei consisting of rock and crust fragments, some nodules do not have nucleus. It is grouped into spherical, flat, platy, and irregular by shape.

(2) Thickness of crusts

The thickness of the crusts and cobble crusts is defined as; the thickness from the surface of the substrate to the crust surface in the direction normal to the layered structure of the crusts. For crust fragments, the thickness is measured also in the direction normal to the layered structure. For cobble crusts with substrate of crust fragments, nuclei of crust fragment are included in the thickness of the crust. The

thickness of the backside, however, is not included.

Regarding the thickness of the nodules, nuclei to the surface is measured for those with nuclei, but short axis is used as thickness for the mono-layered nodules without nuclei.

The average thickness of individual crust-type was calculated by averaging the thickness of samples deemed to represent the type. The average thickness of the total samples was obtained by calculating the weighted average by multiplying the average thickness of each type by its surface area.

(3) Division of the surface structure of the cobalt-rich crusts

The surface structure of the cobalt-rich crusts is classified into the following groups; botryoidal surface which is an aggregate of spherical to oval grains of several millimeters to 10mm in diameter, granular surface which is an aggregate of irregularly shaped minute grains, and smooth surface. Although there are samples intermediate between granular and botryoidal, and also whose botryoidal surface is smoothly covered by crusts and the shape of the grains is not clear, those with clear spherical grains are classified as botryoidal in the present survey.

Generally crusts with botryoidal surface have thick cobalt-rich crusts.

(4)Layers of cobalt-rich crusts

Many cobalt-rich crusts have two- to three-layered structure and some of those thicker than 50mm have more than four layers, and some with irregularly intercalated thin layers can be divided into seven to nine layers.

Structurally the crusts are divided as follows.

- Compact
  - Massive
  - Stratified
    - Non fissile
    - Fissile
- Porous
  - Scoriaceous
    - Prismatic voids developed
    - Spherical voids developed
  - Brick-like
    - Minute voids developed throughout the crusts
    - Minute voids distributed irregularly

Crusts are generally relatively hard, but some scoriaceous materials are soft and can be crushed by fingers. Also some have; intercalations of thin or thread-lace calcite, mixture of iron oxides, ooze and calcareous clay filling the voids, containing iron oxides. All the layers is believed to reflect; the age of cobalt-rich crust, genetic environment, difference of growth rate, and other relevant factors.

Generally with crusts and cobble crusts, thicker crusts tend to have larger number of layers, while nodules tend to be mono-layered. However, there are mono-layered crusts and nodules with several tens of millimeters and also thin crusts and nodules with several layers.

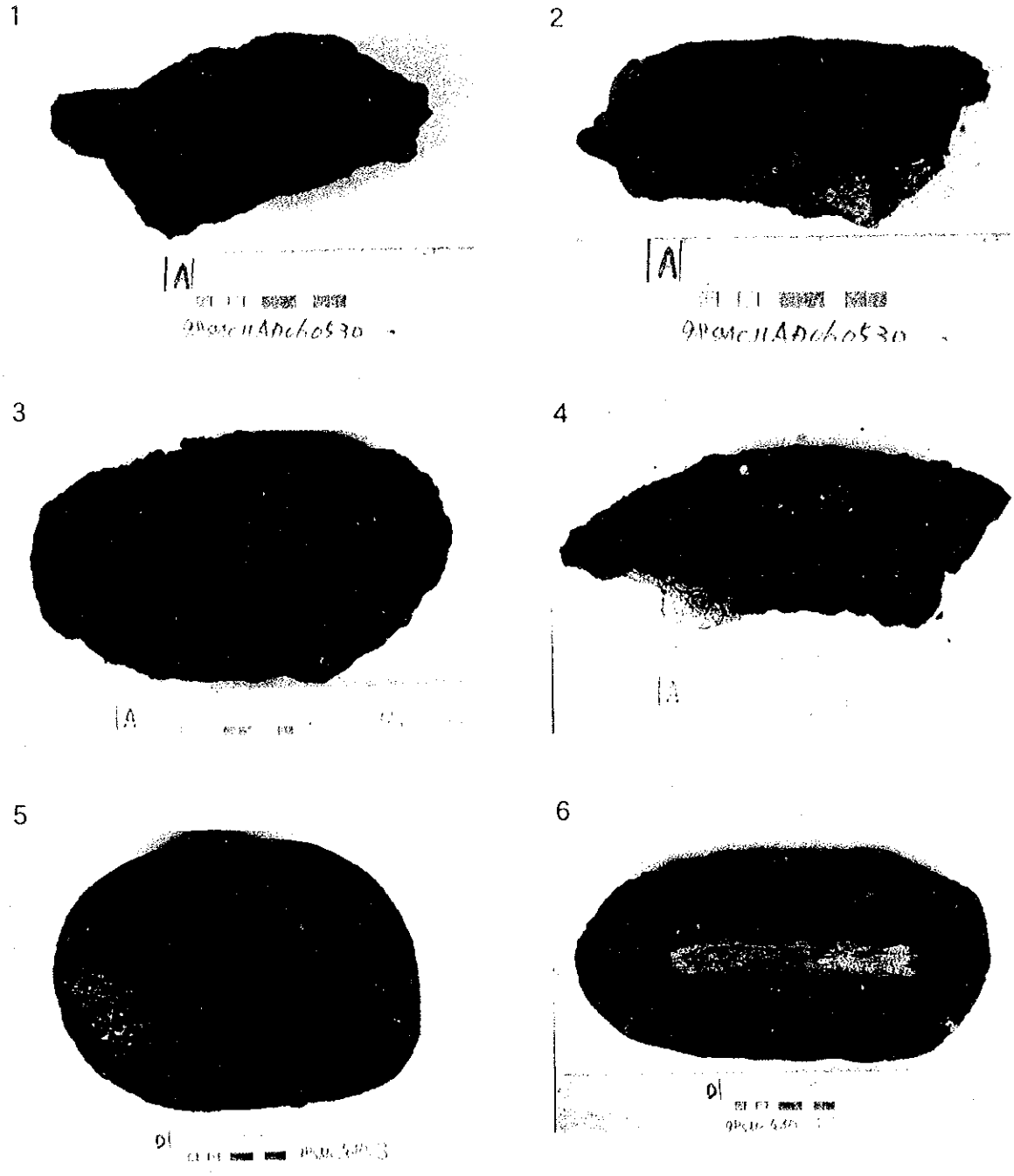

1. 98SMC11AD06-A Crust (upper) surface: granullar
2. " Crust(Section) substrate:Basalt
3. 98SMC12AD08-A Crust (upper) surface: botryoidal
4. " Crust(Section) substrate:Basalt
5. 98SMC12AD08-D Cobble crust (upper) surface: botryoidal
6. " Cobble crust(Section) substrate: Feraminifera limestone

Fig. 5-1-1(1) Photographs of manganese crust

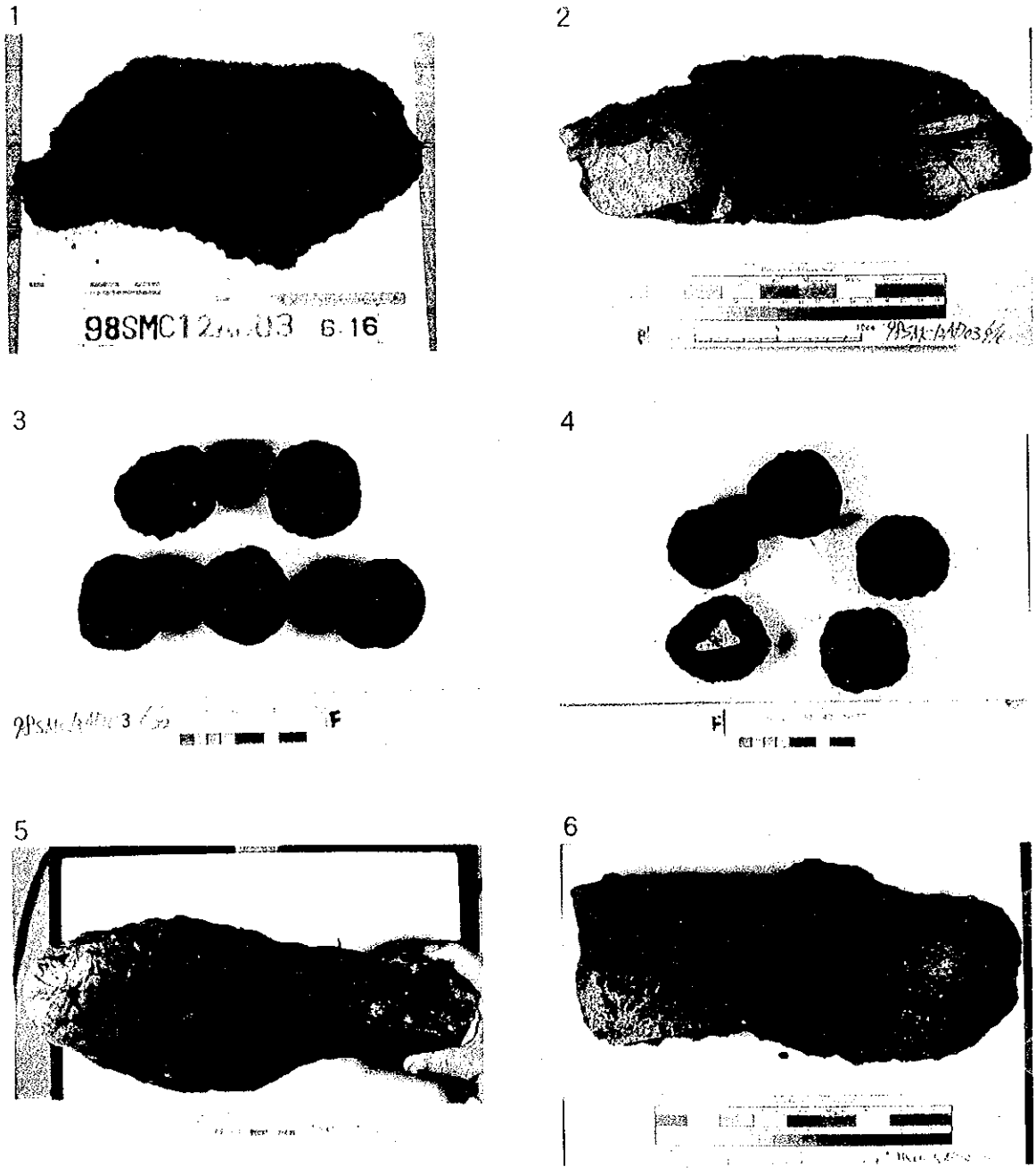

1. 98SMC12AD03-B Cobble Crust (upper) surface: botryoidal
2. 〃 Cobble Crust(Section) substrate: Fragment crust
3. 98SMC13AD03-F Nodule (upper) surface: botryoidal
4. 〃 Nodule (Section) substrate: limestone etc.,
5. 98SMC12AD08-A Fragment crust (upper) surface: botryoidal
6. 〃 Fragment crust(Section)

Fig. 5-1-1(2) Photographs of manganese crust

In the present study, most of the samples were analyzed in bulk, but also in a few cases they each layer was analyzed. The layers are numbered with the outermost layer as the first layer.

5-2 Results of Seafloor Observation (FDC)

TV-mounted deep sea towing camera system (FDC) was used for clarifying the mode of occurrence of the cobalt-rich crusts on the seamounts of each area.

The FDC track lines were designed after considering the results of; MBES acoustic pressure distribution maps, SSS survey results, and sampling by dredges. Clarification of; the mode of occurrence of the crusts, conditions of rock exposures and bottom sediments, and microtopography were the objective of this study.

Five track lines, one to two lines in each of the four areas, MC11~MC13 and MS13 were surveyed.

Representative deep seafloor photographs are shown in Figure 5-2-1(1),(2), FDC survey results in Appended Table 4, FDC route maps (plans and sections) and maps showing the crust exposure ratios are laid out in Appended Figure 5 (1)~(8).

The results of TV camera observation is reported below. The crust exposure ratio is the areal extent of the exposures of the cobalt-rich crusts, cobble crusts, and nodules on the seafloor without unconsolidated cover. It is expressed in percentage of the area surveyed, and it is shown in an average value during 30 second observation. The seafloor area observed by a TV camera is about 3m wide.

<Eastern Sea>

1) MC11 area

One FDC01 track line was surveyed in this area. This track line extends from near the summit (1,750m water depth) of the pinnacle at the eastern part of the seamount to the upper slope (2,820m deep). The length of the track li8ne is 2.1 miles. The results are showing Table 5-2-1 (1).

Crusts with botryoidal surface cover the zone from the pinnacle summit to the upper slope of the seamount. Foraminiferal sand is predominant on the middle to lower slope and observation of the crust is difficult, but the occurrence of cobble crusts has been confirmed.

Small cliffs with relative height of several meters continues from the foot of the pinnacles to the periphery of the summit, and development of crusts with botryoidal surface is observed on the cliff face. Although botryoidal crusts are observed at parts of the shoulder to the upper slope, smooth-surface crusts are predominant in this zone.

2) MS13 area

Two track lines were surveyed. FDC01 extends for 2.2 miles from along the southern pinnacle slope on the summit (1,355~1,970m water depth), and FDC02 extends for 1.7 miles on the northern slope of the seamount. The results are showing Table 5-2-1 (2),(3).

The pinnacle slope in FDC01 is covered by crusts with granular to botryoidal surface. Botryoidal-

Table5-2-1(1) MC11FDC 01 Seafloor Observation Results

A water depth(m)	Topographic division	MBES acoustic pressure	Exposure ratio (%)	Geologic conditions	Crust conditions	Topography
1,750～1,800	Summit	Dark	0～70	Foraminiferal sand cover crusts.	Crust surface botryoidal. Undulating, but relatively smooth topography. Foraminiferal sand cover depressions.	Track line follows topographic contour on pinnacle slope. Several steep cliffs of several meters near 1,800m depth.
1,800～1,930	Summit	Dark	90～95	Crust exposed. Cobble crust scattered on crust.	Crust surface botryoidal.	Pinnacle slope.
1,930～2,050	Summit	Dark	30～60	Foraminiferal sand cover, cobble crust embedded in sand observed.	Cobble crust surface granular.	Middle pinnacle slope.
2,050～2,200	Summit	Pale	0～10	Foraminiferal sand cover.	Some cobble crusts with granular surface. Scattered on seafloor.	Lower pinnacle slope.
2,200～2,300	Summit	Dark	0～40	Crust covered by foraminiferal sand.	Surface botryoidal. Relatively smooth, some undulation. Foraminiferal sand on depression.	Foot of pinnacle
2,300～2,400	Summit	Dark	60～80	Small cliffs continuous and surface covered by crust.	Crust surface botryoidal.	About a dozen or more small cliffs of less than 10m.
2,400～2,700	Summit periphery～ Upper slope	Dark	40～80	Bedrock covered by foraminiferal sand. Angular pebbles deposited rear 2,500m and 2,700m. Probably talus.	Bedrock generally flat. Botryoidal crusts observed locally.	Steep slope probably collapsed cliff.
2,700～2,750	Upper slope	Pale	0	Foraminiferal sand cover.		Ripple marks observed.
2,750～2,800	Upper slope	Pale	10～40	Bedrock covered by foraminiferal sand.	Bedrock surface smooth. crust probably thin, if any.	
2,800～2,850	Upper slope	Pale	0～10	Foraminiferal sand cover.		
2,850～2,855	Upper slope	Pale	5～40	Bedrock covered by foraminiferal sand.	Bedrock surface smooth. crust probably thin, if any.	
2,855～2,820	Upper slope		70～80	Outcrop of bedrock	Bedrock surface smooth. crust probably thin, if any.	Steep cliff.
2,820～3,020	Upper slope	Pale	0～60	Generally covered by foraminiferal sand. Local exposures in parts.	Bedrock surface smooth.	

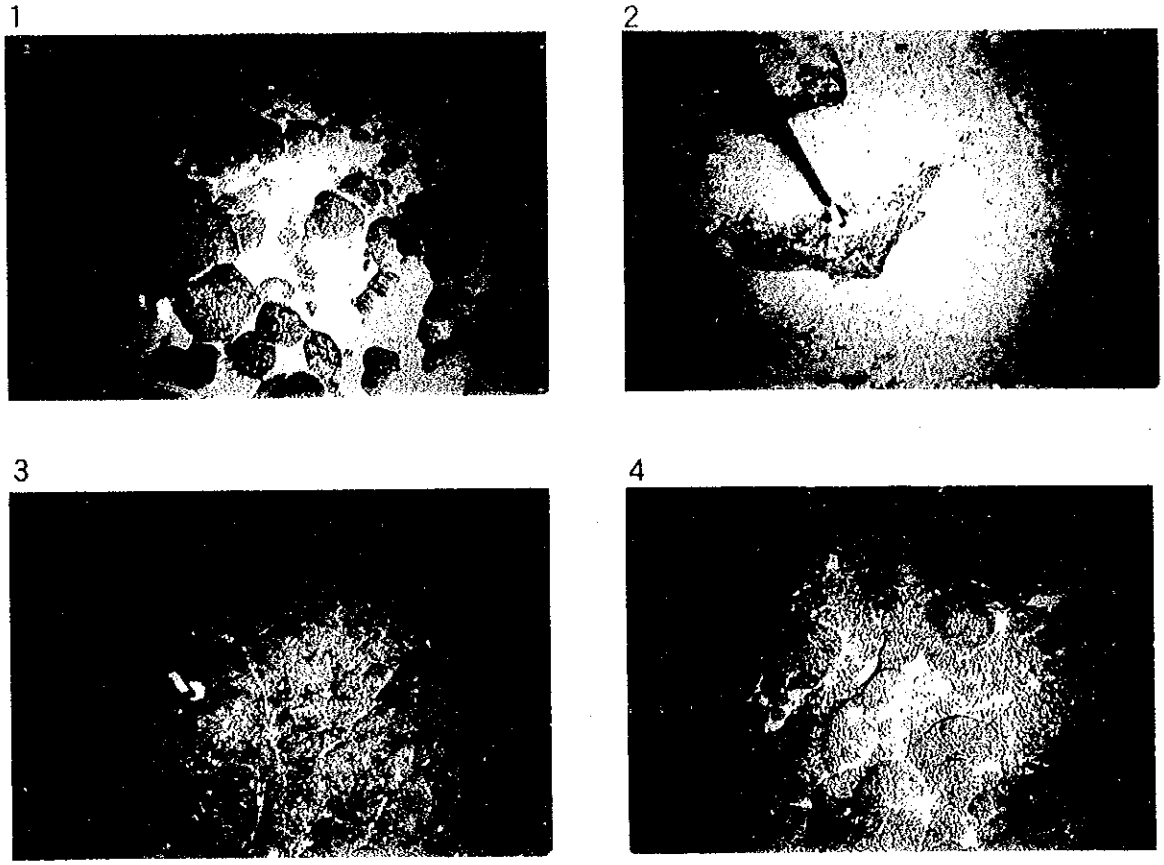

1. 98SMC11FDC01 Cobble crust
   Summit Water depth 2,001m 07° 30.532'N 161° 21.069'E
2. 98SMC11FDC01 Crust covered by foraminiferal sand
   Upper slope Water depth 2,865m 07° 31.061'N 161° 22.309'E
3. 98SMC12FDC01 Crust on slope
   Summit Water depth 1,255m 09° 20.074'N 146° 05.493'E
4. 98SMC12FDC01 Crust with botryoidal surface
   Upper slope Water depth 1,511m 09° 20.341'N 146° 05.798'E

Fig. 5-2-1(1) Photographs of FDC seafloor observation

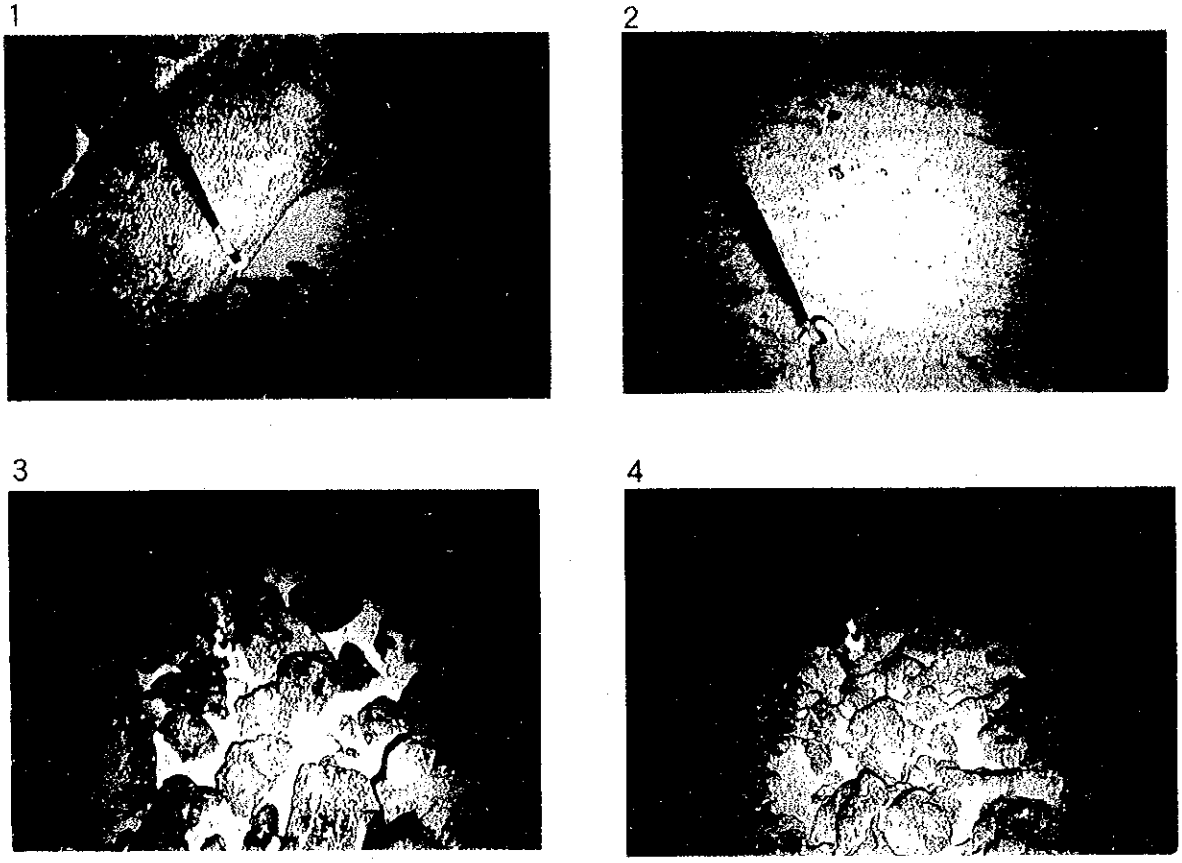

1. 98SMC12FDC01 Crust on an overhunging cliff
   and cobble crust at the bottom
   Upper slope Water depth 1,889m 09° 20.713'N 146° 06.127'E
2. 98SMC12FDC01 Nodules and cobble crust are scattered on the
   foraminiferal sand with ripple mark
   Middle slope Water depth 2,214m 09° 21.042'N 146° 06.488'E
3. 98SMC13FDC01 Cobble crust
   Summit Water depth 2,006m 10° 26.527'N 145° 00.808'E
4. 98SMC13FDC01 Crust with rough surface like lump
   Summit Water depth 2,436m 10° 26.836'N 145° 01.303'E

Fig. 5-2-1(2) Photographs of FDC seafloor observation

Table5-2-1(2) MS13FDC 01 Seafloor Observation Results

A water depth(m)	Topographic division	MBES acoustic	Exposure ratio (%)	Geologic conditions	Crust conditions	Topography
1,430～1,355～1,520	Summit	Dark	20～100	Crusts exposed and covered by foraminiferal sands. Sand deposition is local.	Crust surface partly botryoidal, generally granular. Bedrock stratification observed and crust probably thin.	Pinnacle summits.
1,520～1,610	Summit	Dark	60～90	Crusts exposed, and covered by angular fragments and foraminiferal sands.	Crust surface granular. Angular fragments have clear angles and crusts, if any, are believed to be mere coatings.	Pinnacle slope.
1,610～1,670	Summit	Dark	30～100	Foraminiferal sands cover crusts.	Crusts with granular～botryoidal surface. Bedrock stratification and cracks observed and crusts believed to be thin.	Pinnacle slope.
1,670～1,970	Summit	Intermediate	0～60	Crusts observed in places, but foraminiferal sands cover the general zone and rock fragments and nodules occur sporadically on sand.	Crust surface granular.	Steep cliff over 50m in height.

Table5-2-1(3) MS13FDC 02 Seafloor Observation Results

A water depth(m)	Topographic division	MBES acoustic pressure	Exposure ratio (%)	Geologic conditions	Crust conditions	Topography
2,620～2,670	Summit	Pale	0	Ooze covering seafloor.		
2,670～2,740	Summit periphery	Intermediate	0～90	Ooze covering crust. Ooze generally thin with locally thick spot.	Crust surface botryoidal. Locally granular surface crust occur.	Steep cliff over 10m in height and.botryoidal surface crust one exist on it.
2,740～3,120	Upper slope	Dark	40～90	Generally crust exposing, locally some spot covered with sand. stebut locally. Steep criff which assumed landslide existing and large cobblesoks are scattering.	Generally crust surface botryoidal and granular or smooth surface one exist on the criff. Large cobble are corted with crust.	Generally steep slope and cliff over 50m in height scattering..
3,120～3,200	Upper slope	Dark	0～40	Ooze covering crust.	Generally crust surface botryoida.	Some steep criff assumed landslide.
3,200～3,290	Upper slope	Intermediate	0～5	Ooze covering seafoor widely.	Locally, botryoidal surface crust exposing.	Steep cliff over 50m in height.

surface and cobble crusts with maximum thickness of 60mm and average thickness exceeding 30mm were collected by dredging across the track line.

Crusts and cobble crusts are confirmed at the summit periphery in FDC02 on the northern slope. The topography of the summit periphery consists of a series of stepwise terraces, and crusts with botryoidal surface are distributed on the slope, and cobble crusts occur sporadically on the foraminiferal sand deposited on the terraces.

<Western Sea>

3) MC12 area

One track line 2.1 miles was surveyed in this seamount. It extended from the ridge (1,150m water depth) to the middle part of the northern slope of the Oceanic ridge-type seamount. The results are showing Table 5-2-1 (4).

Crusts are most developed on the ridges of the summit.

Crusts with botryoidal surface occur on the upper slope (below 1,500m water depth) to the middle slope (above 2,300m water depth). Foraminiferal sand is predominant on the gentle slope and cobble crusts and nodules occur on the sediments. Below 2,300m water depth, the track line observed the valley zone and the crust exposure was local and the surface was mostly smooth.

4) MC13 area

One track line was surveyed. It extended for 2.2 miles from the summit periphery (1,660m water depth) to the lower slope (3,200m water depth). The results are showing Table 5-2-1 (5).

Crusts with botryoidal surface are predominant on the ridges of the central part of the summit and cobble crust constitutes the major part of the summit periphery. On the slope, cobble crusts and nodules occur from the upper to middle part, but foraminiferal sand generally covers the area and crusts with botryoidal surface are locally observed. Dredging of this seamount resulted in collecting crusts, cobble crusts and nodules at the summit periphery.

5 - 3 Results of Sampling

Cobalt-rich crusts were sampled at MC11~MC13 and MS13 areas by arm dredge (AD) and large gravity corer (LC). Localities where the MBES images showed high acoustic pressure (high possibility of thin sediments and exposed cobalt-rich crusts on the seafloor) were targeted. The distribution of the sampling sites were designed to clarify the cobalt-rich crust occurrence of the entire seamounts by considering the results of the FDC observation, SBC, SSS, and sampling conditions. Sampling was carried out by the most effective method for each area by considering the characteristics of dredges and corer.

The total number of sampling sites was 49 in four areas; 41 dredge sites and eight corer sites.

The seamounts of these areas have different topographic characteristics and they are; guyot with dome-type summit in MC11, guyot classified as rugged summit in MS13, ridge-type seamount in MC12, and plateau-type seamount in MC13.

Table5-2-1(4) MC12FDC 01 Seafloor Observation Results

A water depth(m)	Topographic division	MBES acoustic pressure	Exposure ratio (%)	Geologic conditions	Crust conditions	Topography
1,160～1,150 ～1,325	Summit	Dark	40～100	Exposed zone over 80%. Many pebbles and nodules.	Bedrock, pebble surface smooth.	Slope relatively undulating.
1,325～1,450	Summit	Dark	0～50	Foraminiferal sands cover bedrock and pebbles.	Bedrock, pebble surface smooth.	Slope relatively smooth.
1,450～1,490	Summit	Dark	30～80	Foraminiferal sands cover bedrock.	Bedrock surface smooth.	
1,490～1,580	Summit	Pale	10～80	Cobble crusts, nodules occur on foraminiferal sands.	Pebbles relatively rounded, surface smooth and crusts probably thick.	
1,580～2,100	Upper slope	Dark	20～80	Foraminiferal sands cover crust surface, cobble crusts and nodules scattered on sand.	Crust, cobble crust surface botryoidal. Relatively smooth, but uneven with foraminiferal sand on depressions.	
2,100～2,200	Middle slope	Pale	0～10	foraminiferal sands.		Ripplemarks, trace fossils.
2,200～2,300	Middle slope	Pale	10～50	Foraminiferal sands cover crust surface, and cobble crusts scattered on the sand.	Crust surface botryoidal. Cobble crust surface smooth.	Slope is relatively rugged.
2,300～2,500	Middle slope	Pale	0～80	Foraminiferal sand cover. Local bedrock exposures, boulders scattered throughout.	Boulder surface generally smooth, but some are granular, somewhat botryoidal.	Ripplemarks, trace fossils not observed.

Table5-2-1(5) MC13FDC 01 Seafloor Observation Results

A water depth(m)	Topographic division	MBES acoustic pressure	Exposure ratio (%)	Geologic conditions	Crust conditions	Topography
1,660～1,700	Summit periphery	Dark	10～80	Exposed zone over 80%. Foraminiferal sands in depressions of fairly flat topography. Many cobble crusts and nodules.	Crust surface botryoidal.	
1,700～2,070	Upper slope	Dark	40～100	Angular pebbles distributed, probably talus.	Angles of pebbles clear and attached crusts are probably thin if any.	Continuous collapsed topography.
2,70～2,300	Upper slope	Dark	25～100	Angular pebbles cover slope, foraminiferal sands cover them. Sands increase with depth.	Anles of pebbles clear and attached crusts are probably thin if any.	
2,300～2,700	Upper slope	Pale	10～35	Cobble crusts scattered on foraminiferal sands. Crusts below the sand exposed locally.	Crusts below foraminiferal sand have botryoidal surface. Cobble crust surface smooth.	
2,700～3,200	Middle ～ lower slope	Pale	0～10	Foraminiferal sand cover, some nodules and cobble crusts occur scattered.	Crust, cobble crust surface smooth.	

Thick crusts were collected from all seamounts, but the mode of occurrence of these crusts differ by the topographic conditions.

Thick crusts exceeding 20mm were collected from; summit periphery and the upper slope of the seamount in MC11, middle to upper slope of the seamount in MC12,
and the vicinity of the pinnacles on the summits of the seamounts in MS13 and MC13.

The nature of the cobalt-rich crusts collected by dredges and corer is summarized for each area below. The sampling sites are shown in Figure 4-2-1(1)~(4). A summary of collected samples is listed in Appended Table 1(1)~(4).

<Eastern Sea>

1) MC11 area

The average thickness of collected crusts and cobble crusts is 36.1mm (excluding nodules) with a maximum of 55mm.

Crusts thicker than 20mm were collected from the vicinity of the ridge-type pinnacles and the eastern summit periphery to the upper eastern slope. Crusts with botryoidal surface were confirmed also at the pinnacle slope and the summit periphery by FDC. Although of poor continuity, crusts with botryoidal surface were also confirmed on the upper slope near 2,700m water depth.
The samples from the northern and southern slope, however, were only coated by manganese oxides, and LC samples from the eastern summit periphery have basalt exposures directly below the foraminiferal sand and crusts have not been confirmed. Thus the distribution of cobalt in this area appears to be localized.

The crusts in this area generally consist of two to three layers, and the first layer is hard and compact, the second porous and somewhat soft, while the third layer is either porous and hard or compact and hard. A few of the samples have porous and hard first layer.

2) MS13 area

The average thickness of collected crusts and cobble crusts is 46.4mm (excluding nodules) with a maximum of 140mm for crusts and 160mm for cobble crusts.

This is a rugged seamount topped by pinnacles, and MBES acoustic pressure images show that, with the exception of near the pinnacles, the summit and the eastern and southern slopes are covered by thick sediments. Sampling was carried out near the pinnacles and the slope on the western and northern side. Thick crusts are concentrated near the summit pinnacles.

Dredging was done at four sites on the slope, only crustal coating was collected at three sites, but FDC seafloor observation confirmed the distribution of crusts with botryoidal surface from the summit periphery to the upper slope. Also 35mm-thick crust and 40mm-thick cobble crust was collected by AD03 on the northwestern side.
Near the pinnacles at the summit, crusts and cobble crusts thicker than 20mm were collected at all sites near the pinnacles. Many samples exceeding 100mm in thickness were collected near the pinnacles on the southwestern part of the summit and the average thickness is over 60mm. Occurrence of crusts was confirmed by FDC even in the vicinity of the pinnacles where dredging could not be carried out. Also

it is inferred from the results of the SBP and SSS surveys that the sediments between the pinnacles are thin, and the existence of consolidated material under the thin calcareous clay was confirmed by LC sampling. Thus the possibility of the occurrence of crusts in this zone is high.
Most crusts and cobble crusts have four-layered structure, and they are; compact first layer, porous second layer, compact third layer, and the fourth layer is very compact with vitreous luster.

<Western Sea>

1) MC12 area

The average thickness of collected crusts and cobble crusts is 40.0mm (excluding nodules) with a maximum of 190mm for crusts and 150mm for cobble crusts.

The seamount in this area is ridge-type and reefal limestone is distributed at the summit with less than 1,430m of water depth. Many samples of crusts and cobble crusts with substrates consisting of reefal limestone and mudstone were collected from this seamount. Of those with reefal limestone substrates, cobble crust collected by AD09 is the thickest with 40mm of crust. However, crusts with reefal limestone and mudstone substrates are generally thin and those exceeding 20mm are rare, and most are in the order of coating.

Thick crusts and cobble crusts were collected along the east-west extending crest on the slope of the ridge-type seamount. Crusts with 20~30mm thickness with basalt substrate were collected at the eastern slope of the ridge. Crusts and cobble crusts with more than 100mm thickness were collected from various parts of the zone from the summit to the middle western slope. The maximum thickness of the samples was 190mm of a crust with hyaloclastite substrate from AD09 (2,474m water depth).

Regarding the northern and southern slopes, crusts and cobble crusts were collected but coated cobbles constitute the major part of the samples. It is observed by FDC that, here, bedrock exposures occur widely above 1,500m of water depth, but the surface is smooth and the crust, if any, would be thin. Below 1,500m water depth, crusts with botryoidal surface are sporadically observed, but the slope is generally covered by foraminiferal sands and the continuity of the crusts is not clear.

The crusts and cobble crusts from the summit are three-layered, and the first layer is compact and hard, the second hard but with fine vesicles, and the third is compact and hard. The crusts exceeding 100mm in thickness from the western slope consist of four to five layers, and the first and second layers have the same characteristics as those from the summit, the third to the fifth layers are porous and fragile, particularly the fourth layer contain a large amount of clay and is fragile with several tens of millimeters thick.

2) MC13 area

The average thickness of collected crusts and cobble crusts is 45.2mm (excluding nodules) with a maximum of 80mm for crusts and 140mm for cobble crusts.

The seamount in this area is a plateau-type composed of steep cliff extending from the northern to the northeastern side and gentle slope widely extending from the western to the southern side. It was confirmed by MBES acoustic survey that the seamount is generally covered by unconsolidated sediments with the exception of the steep cliff and the pinnacles scattered on the northern and eastern parts of the summit.

Thick crusts and cobble crusts occur in the vicinity of the pinnacles on the northern and eastern side of the summit. Crusts are not developed on the steep cliff from the northern to the northeastern side and most of the crusts range from mere coating to several millimeters thick, those exceeding 10mm are rare. By FDC observation, the distribution of crusts with botryoidal surface, cobble crusts, and nodules are confirmed from the pinnacle slope to the shoulder of the steep cliff, but the slope of the steep cliff is covered by angular fragments and foraminiferal sand and the continuity of the observed crusts and cobble crusts is poor.

The thickest crust occurred in cobble crust with crust fragment as the substrate in AD12 collected from the slope of a northern pinnacle. It is 140mm thick. Dredging was carried out at two localities in this vicinity, AD03 and AD12, although crusts were not collected at these sites, both samples contained many cobble crusts and nodules with thick crusts. The substrates are; aside from crust fragments, limestone and mudstone were most common, and basaltic and hyaloclastic pyroclastic rocks were observed as nuclei of nodules.

Both thick crusts and cobble crusts with thick crust were collected near the eastern pinnacles, and the maximum thickness was 80mm for crusts and 105mm for cobble crusts. The substrate of the crusts are foraminiferal calcareous limestone conglomerates, and those for the cobble crusts are foraminiferal calcareous conglomerate, mudstone, basalt, and crust fragments.

Most of the thick crusts and cobble crusts are three-layered, and the first layer is compact and hard, the second layer porous and hard, and the third layer compact and hard. Rarely samples have a hard fourth layer including clay and calcite.

5 - 4 Chemical Composition of Ores

Thirty-seven cobalt-rich crust samples were selected from those collected at 30 sites in four areas of MC11~13 and MS13. They were chemically analyzed. Crusts of eight of these samples were separated into layers and each layer was analyzed, and the relation of the layered crust structure and chemical composition was studied. Total number of analysis was 69 samples.

Samples with thick cobalt-rich crusts were selected for bulk analysis from the crusts and cobble crusts with typical layered structure. As a rule, samples with substrates attached were used, but when crusts and cobble crusts were not available crust fragments and nodules were analyzed.

The results of chemical analysis are laid out in Appendix Table 4 (1),(2).

(1) Analyzed elements and analytical methods

The analyzed elements and analytical methods are shown in Table 5-4-1, and the analyzed elements and the limits of detection in Table 5-4-2. The samples were dried to constant weight before analysis and then the samples were prepared.

Table 5-4-1 Analitical elements and methods

Elements	Methods
Mn, Fe, Ti, Si, Al, Ca, P, Co, Ni, Cu, Pt	ICP emission spectrometry
Pb, Zn, V, La, Ce, Pr, Nb, Sm, Eu, Gd, Tb, Dy, Ho, Er, Tm, Yb, Lu	ICP mass spectrometry

Table 5-4-2 Analyzed elements and limits of detection

Elements	Limits of detection
Co, Ni, Cu, Mn, Fe, Pb, Zn, Ti, Mo, V, Si, Al, Ca, P	0.01%
Pt, Pd, La, Ce, Pr, Nb, Sm, Eu, Gd, Tb, Dy, Ho, Er, Tm, Yb, Lu	0.1ppm

(2) Chemical composition

The results of analysis of five major elements and platinum, and rare earth elements of the samples from various areas are laid out in Table 5-4-3. A radar chart of the five major components of the cobalt-rich crusts are shown in Figure 5-4-1.

Different tendency is observed between the results in MC11 and MS13 areas of the Eastern Sea and that f the MC12 and MC13 areas of the Western Sea. Namely the average grades of Co, Ni, and Mn are high in MC11 and MS13 areas of the Eastern Sea, while they are low in MC12 and MC13 areas of the Western Sea. C0 content is particularly low in MC13 area and Ni content is low in MC12 area. The Mn grade is 2.5~4.5% lower in the two areas of Western Sea compared to Eastern Sea areas. But Cu and Fe grades are higher in Western Sea, Fe content is 4~5.5% higher. Also high copper grade samples were recovered from MC12 area.

The chemical characteristics of the cobalt-rich crusts of the four areas surveyed are summarized as follows. The relation between the water depth of the sampling site and the grade is shown in Figure 5-4-2.

- Co grade varies considerably by the sampling site in all seamounts. Co grade of the cobalt-rich crusts generally tends to increase with the decrease of water depth, but in the present survey area, this trend was observed only in the mC12 area.
- Ni grade also varies considerably in all areas with the exception of MC11 area. The grade tends to

decrease with water depth.

- Cu grade varies considerably by the sampling sites in all seamounts. Content of some samples was below the limit of detection. Correlation between the water depth and grade is not observed. Samples containing three times the average Cu grade were obtained in Mc12 area, and these are nodules from the lower slope.
- Mn grade differs significantly between the two sea areas. Although the grade varies by the sampling sites, the grade tends to decrease with water depth.
- Fe average grade tends to increase with water depth, but the correlation is weak.
- Variation of Pb, Zn, Ti, Mo, V grades by sampling sites are relatively small. The Pb, Zn, Mo grades of samples from lower slope and the foot of seamounts are low, and it is noted that Pb and Zn grades tend to decrease with water depth.
- Pt grade varies considerably by sampling sites. The grade tends somewhat .To decrease with water depth.
- Grades of the rare earth elements, with the exception of Ce, do not vary in the four areas, and the difference of the Ce grade becomes the difference of total REE content. Correlation between the grade and water depth is not observed.

(3) Local characteristics

Chemical characteristics of cobalt-rich crusts by areas are summarized below.

- MC11 area has the highest Co, Ni, Mn grades among the four areas.
- MC12 area has the highest Cu, Fe grades among the four areas. Also Pb, Zn, Ti, Mo, V gradesareighest among the four seamounts. Co, Ni grades are also high, and some samples have high Pt grade.
- MC13 area has the lowest Co, Mn, total REE grade among the four areas. The Pb, Zn, Ti, Mo, V grades of this area, however, are not different from those of other areas. Some samples have high Ni grade.
- MS13 area has the highest Pt, total REE grades among the four areas. Co, Ni, Mn grades are also high.

(3) Results of layer analysis

Of the samples analyzed chemically, each layer of eight samples was analyzed separately. Samples with three to six layers were used. The average grades of the layers are laid out in Table 5-4-4.

Co, Ni, Mn grades of cobalt-rich crusts generally tend to increase outward from the inner layer and Cu and total REE contents tend to decrease outward. The samples analyzed in this survey do not have this tendency. But by dividing the layers into compact ones and porous layers, Co, Ni, Mn grades are higher in the outer layers and Cu grade tends to be lower. Similar trend is observed between the compact and porous layers, and Pt grade of porous layers tend to be higher.

Table 5-4-3 Results of Crust analysis

Area	Co %	Ni %	Cu %	Mn %	Fe %	Pt ppm	total REE ppm	Mn/Fe
MC11 area ave.	0.612	0.430	0.039	23.506	17.156	0.263	1628	1.372
MC12 area ave.	0.376	0.268	0.051	17.650	19.653	0.268	1331	0.918
MC13 area ave.	0.366	0.291	0.044	17.708	19.725	0.219	1428	0.907
MS13 area ave.	0.502	0.387	0.039	20.751	16.872	0.365	1650	1.242
MC area ave.	0.426	0.332	0.041	19.084	18.670	0.265	1419	1.044

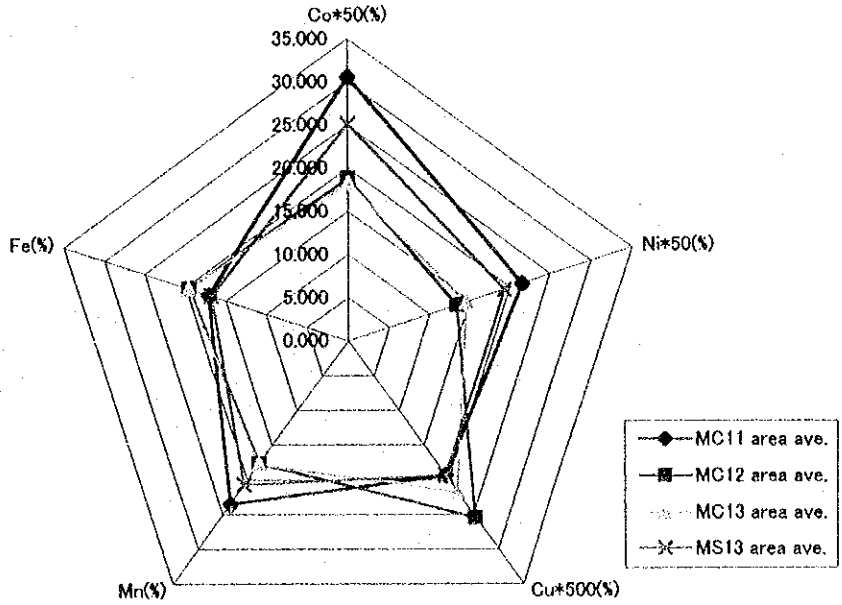

Fig.5-4-1 Comparison of five principal components

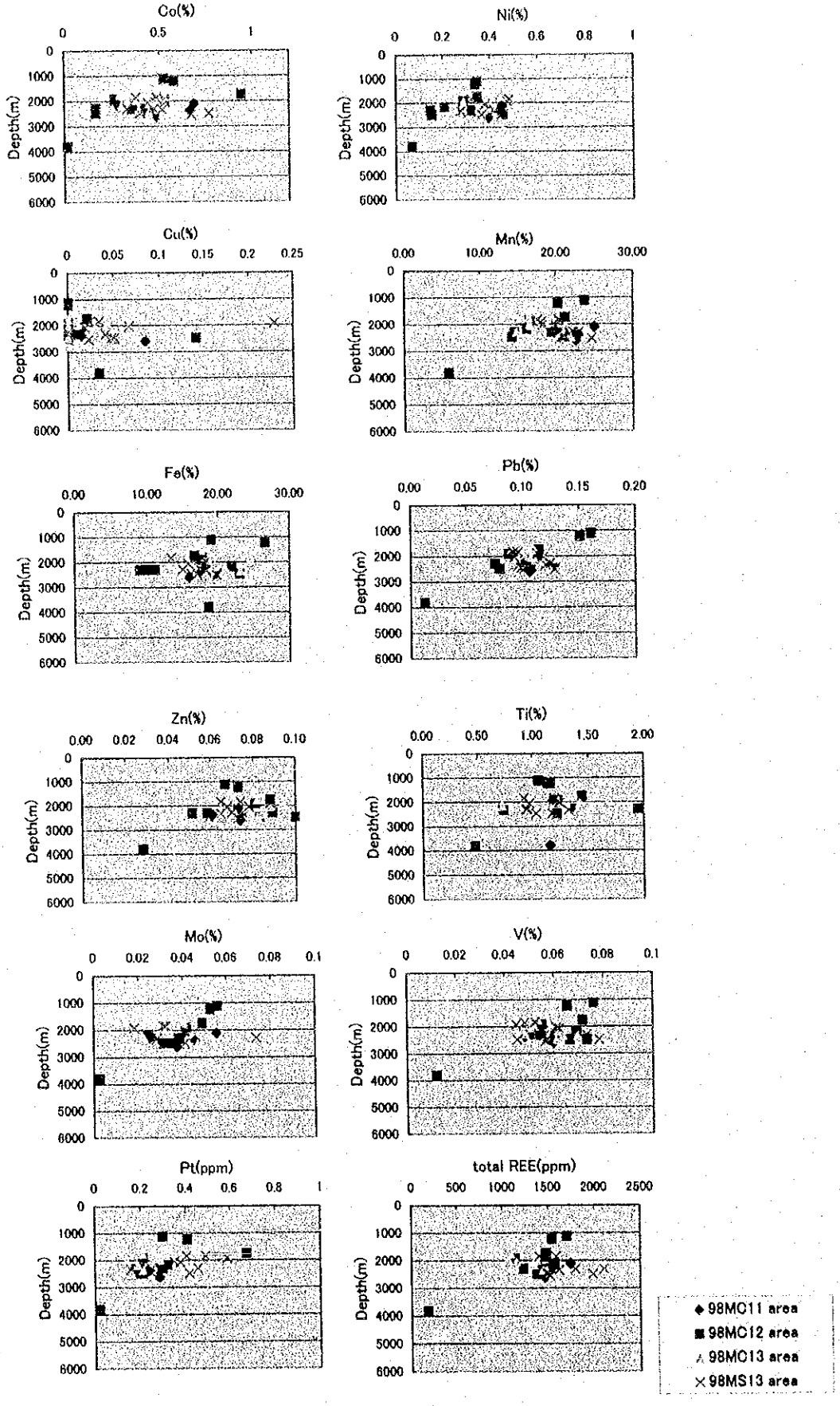

Fig.5-4-2 Sampling depth and concentration of each element

Table 5-4-4 Results of layer analysis

Layer	Co %	Ni %	Cu %	Mn %	Fe %	Pb %	Zn %	Ti %	Mo %	V %	Si %	Al %	Ca %	P %	Pt ppm	total REE ppm
First layer	0.986	0.546	0.019	26.06	14.08	0.15	0.07	0.86	0.064	0.058	2.44	0.52	3.06	0.55	0.26	400
close	1.002	0.554	0.012	26.60	14.13	0.16	0.07	0.84	0.066	0.060	2.26	0.46	3.23	0.61	0.25	406
porous	0.918	0.512	0.069	23.71	13.85	0.13	0.06	0.94	0.052	0.050	3.25	0.76	2.34	0.29	0.29	372
Second layer	0.623	0.500	0.030	23.80	16.04	0.14	0.08	1.09	0.049	0.058	2.68	0.70	4.37	1.06	0.49	403
close	0.700	0.555	0.038	25.44	15.33	0.15	0.08	1.03	0.061	0.061	2.15	0.50	4.07	0.91	0.44	424
porous	0.564	0.458	0.024	22.56	16.57	0.14	0.07	1.13	0.041	0.056	3.08	0.85	4.58	1.18	0.52	387
Third layer	0.599	0.580	0.051	24.54	13.65	0.12	0.08	0.91	0.061	0.058	1.90	0.53	4.89	1.12	0.42	432
close	0.599	0.600	0.047	25.23	13.45	0.12	0.08	0.85	0.066	0.060	1.42	0.36	5.27	1.26	0.37	448
porous	0.600	0.518	0.062	22.47	14.25	0.10	0.08	1.11	0.045	0.052	3.32	1.04	3.76	0.70	0.58	386
Fourth layer	0.352	0.454	0.069	19.94	12.45	0.10	0.07	0.63	0.056	0.056	1.47	0.43	10.24	2.82	0.52	423
close	0.359	0.489	0.063	20.57	11.94	0.10	0.07	0.61	0.059	0.056	1.30	0.38	10.40	2.78	0.46	416
porous	0.332	0.348	0.086	18.03	13.96	0.09	0.07	0.70	0.046	0.055	2.00	0.59	9.74	2.96	0.69	443
Fifth layer	0.329	0.427	0.060	21.08	12.28	0.12	0.07	0.77	0.051	0.057	1.78	0.49	10.22	2.98	0.39	413
Sixth layer	0.212	0.259	0.050	15.35	12.72	0.13	0.06	0.67	0.040	0.056	1.58	0.41	13.70	4.42	0.35	428
Seventh layer	0.370	0.437	0.062	20.86	10.29	0.12	0.08	0.66	0.048	0.053	1.32	0.41	12.99	3.20	0.51	487

5 - 5 Identification of Branching Corals and ^{14}C Age Determination

Coral community coated by cobalt-rich crusts was collected from MC12 seamount slope at about 1,200m water depth. Attempts were made to infer the period and environment of the coral growth through identification of species and ^{14}C age determination of these coral samples, and thereby acquire data concerning the environment and also the rate of cobalt-rich crust growth.

The samples used for this investigation are three in AD09 from 1,068~1,091m depth, and one in AD05 from 1,203~1,254m water depth.

<Results of coral identification>

Characteristics for identifying the species could not be observed on the branching corals in AD05, but the coral in AD09 were judged to belong to Anthozoa Hexacorallia Scleractinia. Also the collected samples have been coated with manganese oxides and decalcified, and thus it was not possible to determine the genus and species, but from the frame, structure, and other features it is inferred to be of species close to genus Archohelia of family Oculiniae of order Scleractinia. However Archohelia is a non-reef-building coral in deep seas of the Atlantic Ocean and the genus became extinct in Pliocene.

Cobalt-rich crust coating can be observed along the growth lines on the sections of the samples. This indicates that coral growth was interrupted, coated by manganese oxides, and then resumed growing. Also the branches are intact with no trace of breakage or abrasion. And thus the possibility of their growth in other areas and transportation to the present sites is very small. From the above it is concluded that the growth environment of these corals was the deep seafloor where cobalt-rich crusts were formed, and that the summit of the seamount of MC12 area was at such depth during the period of coral growth.

<^{14}C age determination>

The samples were cleaned; namely cobalt-rich crust coatings and deteriorated carbonate minerals were removed, and prepared for measurements.

Accelerated mass spectroscopy (AMS) was applied, calibrated for CO2 exchange between atmosphere and sea water and isotope discrimination effect by using PDB-standard (belemnite fossil).

Considering the low supply of 14 in deep sea environment, the measured values could be somewhat on the larger side, but the error is believed to be in the vicinity of 100 years. The measured results are laid out in Table 5-5-1.

Table 5-5-1 Results of ^{14}C age determination

	δ 14C(‰)	δ 13C(‰)	Δ14C(‰)	RADiocarbon Age (BP)
SMC12AD05	-916±1.3	-8.1	-918.9±1.3	20130±130
SMC12AD09	-846.3±1.5	-0.4	-853.8±1.5	15398±80

<Growth rate of cobalt-rich crusts>

The collected coral community is believed to have stopped growing by factors such as the change in sea water temperature at around 20,000 to 15,000 BP, and its surface began to be coated with cobalt-rich crusts. The coating is 0.1mm thick for samples from AD05 and 0.1~0.2mm in samples from AD09. This thickness is believed to be the result of manganese oxide growth during the past 15,000~20,000 years. The rate of growth would be 5~10mm/Ma. The rate of growth of 30~40mm-thick outer layer of cobalt-rich crust was measured on samples collected in the present seas during the past year by 10Be method and the result was 1.4~7.1mm/Ma, Sharma and Somauajulu (1982) maintains that the growth rate of cobalt-rich crusts of the Pacific area to be 1~8mm. The figures acquired on cobalt-rich crust growth rate in the course of the present study is relatively large.

5 - 6 Conditions of Cobalt-rich Crust Occurrence

The characteristics of the occurrence of cobalt-rich crusts in this area is summarized as follows from the results of the survey carried out in Fiscal 1997 and this year.

The occurrence of cobalt-rich crusts vary widely by area. The average crust thickness exceeds 20mm in the seamounts in the northern part namely; MC02, MC08, MC10, MC11, MC12, MC13, and MS13 areas, and those exceeding 100mm were collected from seamounts in four areas. On the other hand, exposure ratio is good but the average thickness of the crusts is thin at 1 to several millimeters on the seamounts in the southern part namely; MC05, MC06, MC07, and MC09 areas.

The relation between the occurrence of cobalt-rich crusts and topography・geology is summarized as follows.

・Seamounts older than Paleogene (MC08, MC10, MC11, MC12, MC13, and MS13 areas) have thick

crusts developed, while the younger seamounts (MC04, MC05, MC06, MC07, and MC09 areas) have thin crusts.

- The thickness of crusts on seamounts younger than Paleogene are influenced more by topography and geology than by age.
- Crusts on pointed seamounts (MC04, MC05 areas) with shallow summit are very thin.
- Areal differences are also observed on the average metal grade of the major components. Cu content is higher, and Co and Mn lower in MC02, MC08, MC10 areas than in other areas. The average cobalt content is high at 0.51~0.61% in the northeastern seamounts of the area adjacent to the EEZ of the Marshall Islands, while it is low at 0.35~0.41% in the seamounts in the northern part of the western area, and that in southern seamounts is also low at 0.38~0.48%.

Assessing the seamounts on the basis of the crust occurrence; MC11 and MS13 areas adjacent to the Marshall Islands EEZ with high Co, Ni, and Mn grade and thick crusts and cobble crusts are the most promising, followed by MC12 and MC13 areas. Old seamounts are generally promising.

The mode of occurrence of cobalt-rich crusts in areas surveyed this year are summarized in Table 5-6-1.

Table 5-6-1 Characteristic of occurrence of manganese crust

Area	Scale of seamount	Topographic of seamount			Crust exposure		Crust thickness(mm)		Average		
		Riughness	Gradient of flank	Depth of summit	Summit	Flank	maximum	Average	Co(%)	Ni(%)	Pt(ppm)
MC11	small	a little	11°	1,777m	low	low	55	36.1	0.61	0.43	0.26
MC12	big	a little	15°	1,114m	high	high	190	40.0	0.38	0.27	0.27
MC13	big	a little	8°	1,656m	low	high	140	45.2	0.37	0.29	0.22
MS13	big	much	7°	1,387m	low	low	160	46.4	0.50	0.39	0.37

- In MC11 area, Cu, Ni, Mn grades are higher than other areas of the area. But the crust exposure ratio is low, and the distribution of thick crusts are irregular.
- In MC12 area, the major metal content is rather low in this area with the exception of slightly high Cu. But thick crusts and cobble crusts have been confirmed, and the thickest crust (190mm) in the whole survey area was collected from this area. Crust exposure ratio is also high. The crust thickness, however, varies widely on the seamount.
- In MC13 area, the ore grade is the lowest of the four areas surveyed this year. It is also rather low in rms of the entire marine area, but thick crusts and cobble crusts occur and the average is highest in this survey area at 45.2mm. But as in the case of MC12 seamount, the distribution of crust thickness is irregular.

- The MS13 seamount has slightly lower metal grade than the MC11 seamount, but the Cu, Ni, Mn grade is high compared to that of other areas of the survey area. It is highly possible that thick crusts occur throughout the seamount, but it is generally covered by sediments and the thick crust distribution confirmed this year is limited.

Chapter 6 Hydrothermal Activity

MC02 area is located in the central part of the Caroline Ridge, and the seamount is a plateau-type with a group of pinnacles at the southeastern part of a plateau-type high. The shallowest summit of the pinnacles is 1,080m of water depth. A trench topography is observed on the northern side of the seamount and it has an east-west extending axis which is the same direction as the Eauripik Trough and crosses obliquely with the extension of the Caroline Ridge and Sorol Trough direction. This trench extends for 60nmi and is more than 3,000m deep from the sea surface. A depression extending in the WNW-ESE direction was discovered within this trench topography during the last year survey. This direction is the same as that of the Sorol Trough. Also pyrite dissemination was observed in parts of the basalt and pyroclastic samples collected at AD03 which is at the lower northern slope of the seamount and is close to the intersection of the above two fissures and is 3,335m from the sea surface. Pyrite-chalcopyrite dissemination was also discovered at almost the same location by USGS-KORDI team in 1992. This fact suggests the existence of present or past hydrothermal activity in the area. Based on these findings, it was decided to investigate the conditions of hydrothermal activity in the MC02 area this year.

6 - 1 Topographic Survey

(1) Outline of topography

The MC02 area is located in the central part of the Caroline Ridge in western Caroline Islands. It is somewhat to the east of the intersection of the Caroline Islands and the Yap Islands. Carolines extend in the east-west direction while the Yaps in the north-south. The northern side of the MC02 is contiguous to the western edge of the Mariana Basin and the Mariana Trench is further north. The southern side is adjacent to the Sorol Trough, and Eauripik Trough, Caroline Basin, and the Solomon Islands (New Hebrides Arc) lies further south. The direction of the axis of arrangement of the oceanic ridges, island arcs, trenches, and troughs are as follows. Caroline Ridge, Sorol Trough, and the parallel ridge topography on the southern side have WNW-ESE trending axis; Challenger Deep of the Mariana Basin, depression in the MC02 area, Eauripik Trough, and the central part of the Caroline Islands have approximately E-W trending axis.

The seamount of the MC02 area constitutes a part of the high in the central part of the east-west trending plateau of the Caroline Ridge. And the northern side of the seamount is a steep cliff extending linearly in the east-west direction and the southern side forms a gentle slope.

The bird's eye view of MC02 area is shown in Figure 6-1-1 and topological map of seafoor shown in Appendix Figure 2(5).

The inclination of the steep slope on the northern side is 35 ° in average with a maximum of 59 ° and the shoulder of the slope is 1,900m from the base.

The summit is a wide gentle slope dropping southward with 2 ° inclination and it is not possible to distinguish the summit and the slope from topographic inclination alone. In this report, the shoulder of the northern steep slope is defined as the border between the summit and slope, it is 1,400m in water depth. Group of pinnacles occur in an east-west trending gentle arc in the southeastern part of the

summit. The relative height of these pinnacles is around 500m. The shallowest part of the seamount is these pinnacles and the water depth is 1,080m.

The northern slope of this seamount continues to a depression near the central part of the Caroline Ridge. This depression extends 80nmi and is 10~15nmi wide. The map of MC02 covers about 40nmi of this trench in its central part. There is a gently inclining deepest depression with east-west axis, parallel to the depression, at the base of the slope of the trench. A 350m deep graben-type depression occurs around 9° 13.5'N, 141° 34.5' E in the central part of the trench to the north of the above depression. Linear valley topography continues from this graben center for over 40nmi in the WNW-ESE direction. Further to the north, small scale ridge-valley arrangement is observed whose axis direction is similar to that of the central valley topography, and the bottom of the depression gently becomes shallow northward.

(2) MBES Acoustic Intensity Distribution Map

Acoustic reflection intensity distribution is sown Figure 6-1-2.

Dark parts are distributed in the images corresponding to the northern steep slope indicating exposed bedrock on the whole slope. The summit, on the other hand, is covered generally by pale-colored parts from the central part to the shoulder of thenorthern slope, with the exception of the vicinity of the pinnacles. This indicates the unconsolidated sediment cover of the summit of this seamount. Dark belt of the image are arranged in an arc in accordance with the row of pinnacles in the southeastern part indicating exposed bedrock. The uplifted part in the southwestern part of the summit is also shown in dark color and it is inferred that the unconsolidated sediments are thin with exposed rocks in some parts.

The depression is generally covered by pale tone and indicates the wide cover of unconsolidated sediments, but it darkens toward the slope base on the southern side of 9° 15' N suggesting the coarser-grains of the sediments. Dark parts・unreflected parts extend in a dotted line in the east-west・northwest-southeast direction and it is believed that this reflects the structure of the valley-type topography.

(3) SBP Survey

With the exception of the pinnacles, around 10m thick transparent layers are observed on the summit, and this is believed to correspond to the distribution of unconsolidated sediments. In the central part where it becomes shallow, the sediments locally exceed 20m in thickness. The pinnacle parts are shown in opaque layers and is believed to represent exposed bedrocks.

In the depression on the northern side, transparent layers generally cover the acoustic basement. The transparent layers are relatively thin at 10~20m to the vicinity of 9° 15' N from the slope base, but the thickness tends to 20~50m to the north of 9° 15'N. For exsample, SBP profile image of 9° 13'N survey line is shouwn in Figure 6-1-3.

(4) SSS Survey

Two track lines were arranged in order to confirm the mound-type topography and the distribution of

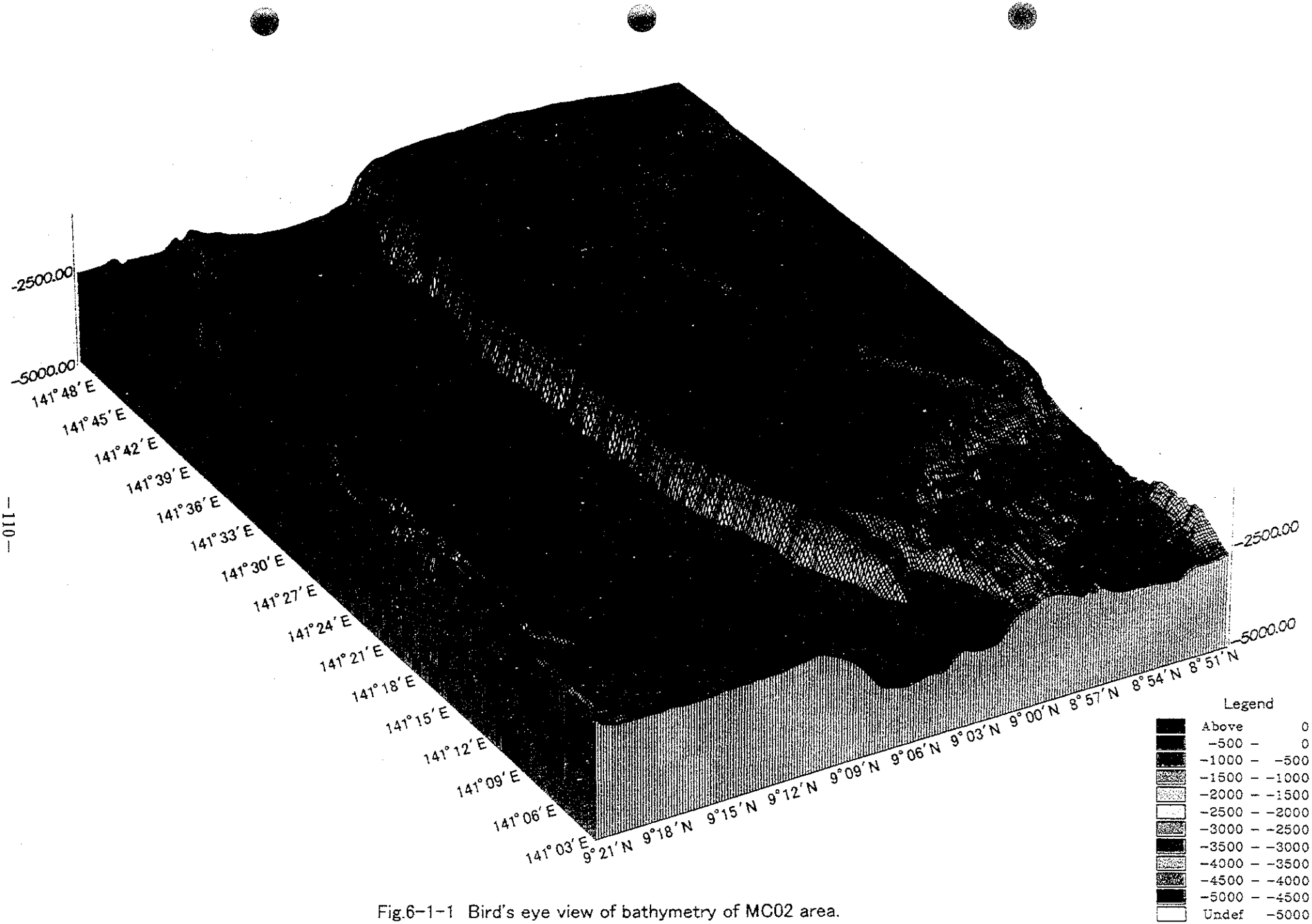

Fig.6-1-1 Bird's eye view of bathymetry of MC02 area.

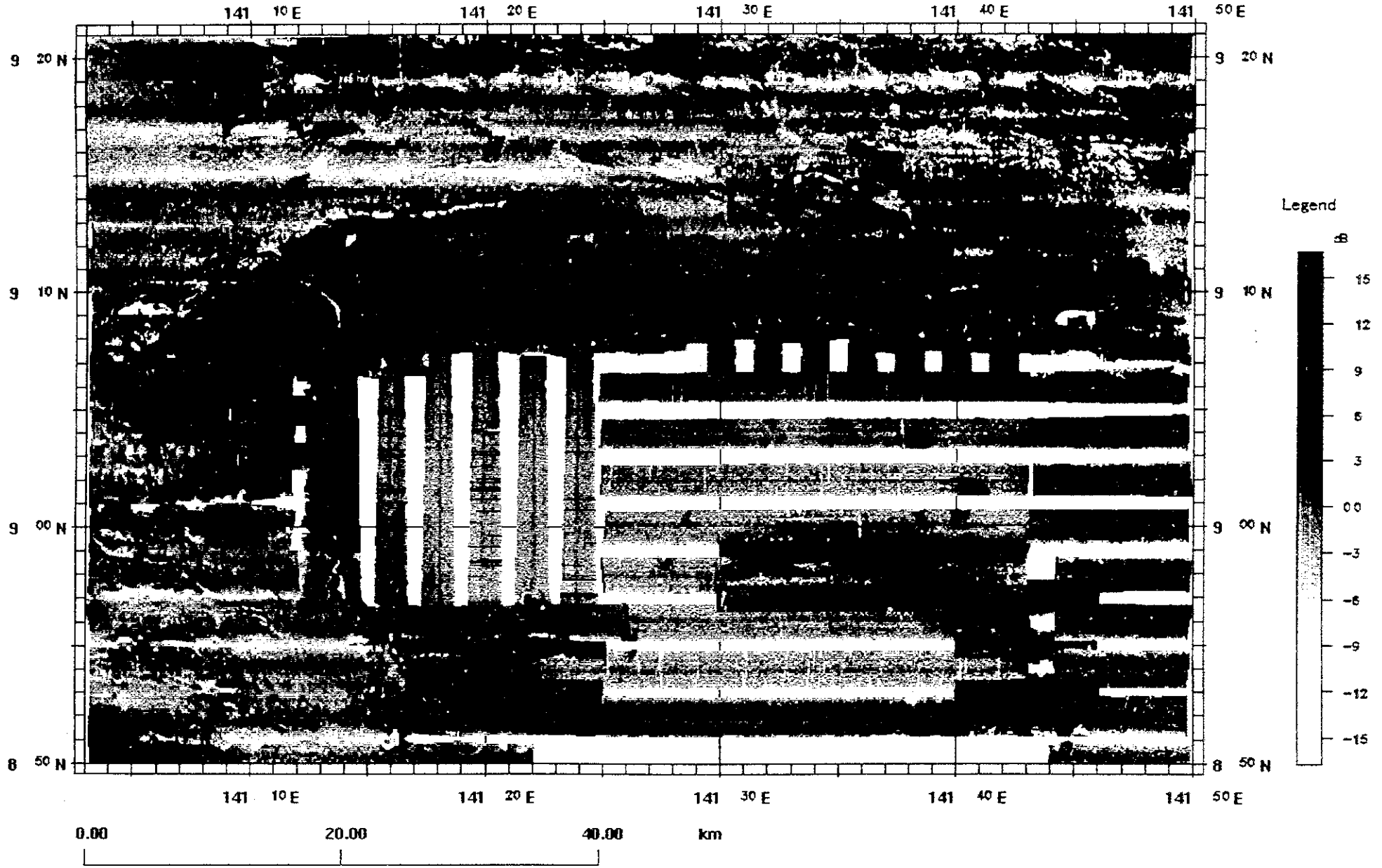

Fig.6-1-2 Acoustic reflection intensity distribution of MC02 area.

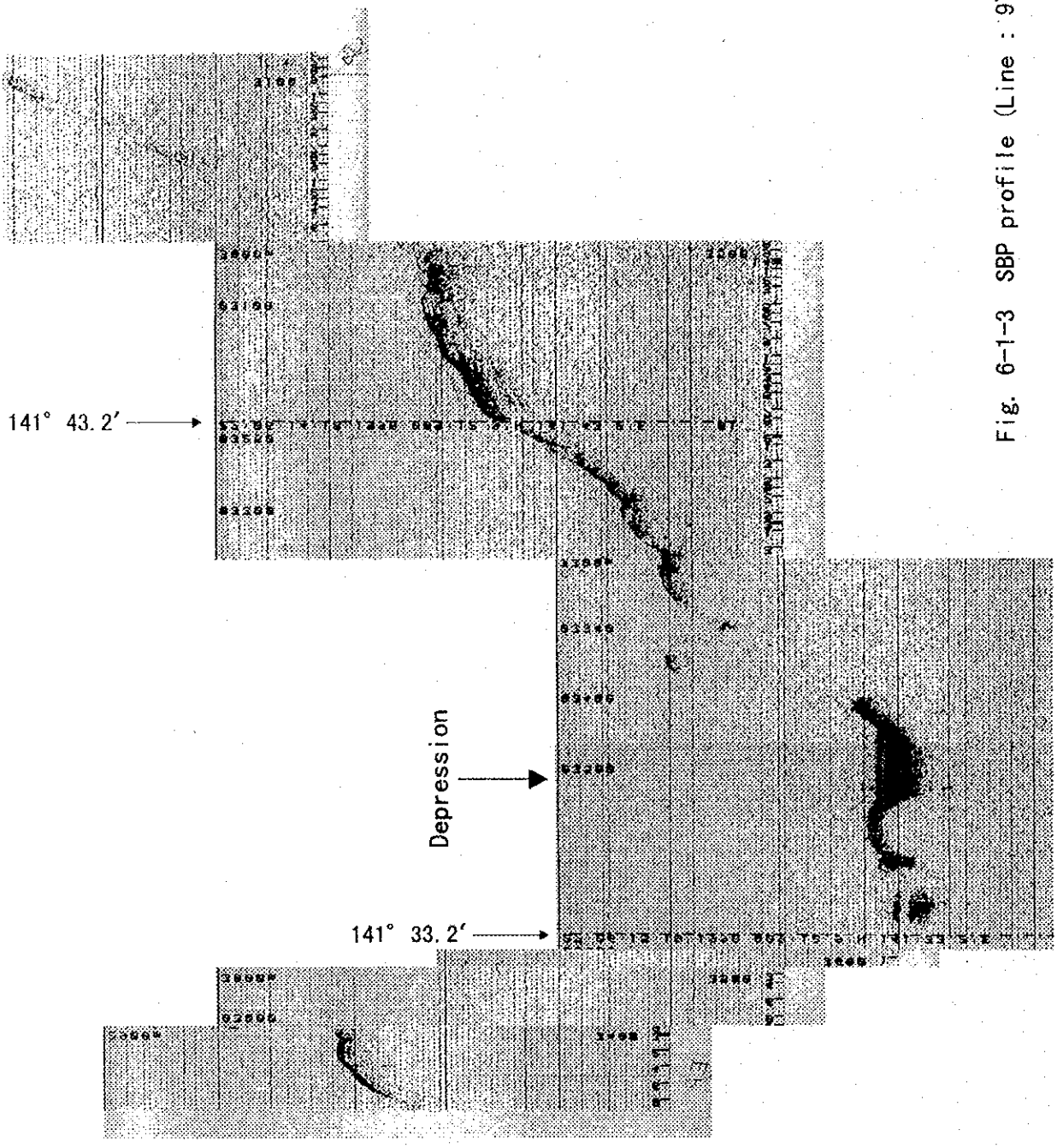

Fig. 6-1-3 SBP profile (Line : 9° 13′)

exposed bedrocks around the small diamond-shaped depression near the intersection of the E-W and ESE-WNW trending linear structures in the trench.

The SSS image is shown in Figure 6-1-4.

At this small depression, a track line was set for 5.2nmi from the northwestern end to the central part of the depression. The SSS image showed the wide distribution of low reflection indicating unconsolidated sediments at all the localities of; the slope of the northwestern end - terrace at the middle step - the slope to the bottom of the depression. Thus the whole image consists of pale color. There is a locality at the bottom of the depression where slightly dark tone prevails indicating the thin coverage of the unconsolidated sediments over the bedrock.

Gentle highs are distributed between the small depression and the base of the seamount. The base of the slope is a gentle E-W trending depression due to these highs, and samples indicating hydrothermal activity were collected at the lower slope of the seamount in this part during the previous cruise. Therefore, a track line extending for 6nmi in the E-W direction was set at the base of this slope. The SSS image generally showed pale tone indicating the prevailing amount of unconsolidated sediments. On this track line, dark parts indicating the reflection from cobbles were obtained at 141° 33'~ 34' E, and the existence of more than a dozen 10m diameter and 10m high "mounds" were recorded. Also record inferred to be a talus deposits was obtained near 141° 31'E.

6 - 2 Geology

(1) Outline of Geology

The spreading of the Caroline Basin is inferred to be about 33~20Ma from the magnetic banding. The spreading axis extends in the W-E direction and thus the majority of the W-E trending linear structures near the Caroline Ridge are believed to have been formed at the time of the opening. During the 1997 cruise. a relatively young basalt of 10~13Ma was obtained from a seamount at the northern edge of Caroline Basin, namely on the southern side of the present survey area. From these data, the existence of a younger linear structure with WNW-ESE or NW-SE trend is suggested. The distribution of a younger valley structure with WNW-ESE trend within the E-W trending trench in the MC02 area support the above hypothesis.

Chemical analysis of the basalt from the slope showed that it is a plume-type mid-oceanic ridge basalt (PMORB). Also K-Ar dating provides a reference age of 22Ma for the rock. The basalt from the seamounts in the vicinity are oceanic island alkaline basalt (OIA), oceanic island tholeite (OIT), and island arc tholeite (IAT). PMORB was collected only from the MC02 area, confirming the possibility of mid-oceanic ridge type hydrothermal activity in this part.

It is believed that the Caroline Ridge was formed before the PMORB activity, but samples fit for age determination could not be obtained from other basalt and reefal limestones. The foraminifera from bottom sediments show that they are from late Miocene. Thus it is inferred that the seamount was formed before Miocene, coral reef was formed on the summit, and the summit was submerged after late Miocene.

(2) Results of FDC observation

FDC observation was carried out over three track lines in this area. They are; FDC01 extending over the mound-like protrusions found by SSS survey at the base of the slope, FDC03 and FDC02 over the talus deposits near 141° 31'E and 141° 33'E extending from the lower slope to the base respectively.

The location maps of FDC are shown in Figure 6-2-1(1),(2), and phptographs of typical seafloor shown in Fifure 6-2-2. Summary of FDC survey is attached in Appendix Table 4 and Rout maps of FDC also shown in Appendix Figure 5(6)~(8).

The mound-like protrusions, which were confirmed by SSS survey, were observed at four localities. It was observed, here, that protrusions exceeding several meters consist of pillow lava within the deposited foraminiferal sand. Also it was confirmed that they are distributed as independent small mounds. In other parts of the base of the slope, an larger protrusion exceeding a dozen meters in relative height is recorded on NBS chart and this is inferred to be a similar occurrence.

The FDC02 and FDC03 track lines observed the talus deposits below the point where basalt with pyrite dissemination was dredged. Distribution of many angular fragments covered by foraminiferal sand was confirmed in this zone.

(3) Results of sampling

Rock and unconsolidated sediments were sampled by arm dredge, chain bag dredge, and large corer was carried out at the trench-type zone this year. Total number of sampling sites amount to eight including dredging and large corer sampling at four sites each. The location of the sampling sites are shown in Figure 6-2-3 and the results in Appended Table 1 (2). The photographs of typical sampled rocks are shown in Figure 6-2-4(1),(2).

The collected samples are briefly described below.

1) Rocks

a. Basalt

Angular fragments of basalt was dredged at all four sites. It is generally chloritized. Fresh samples are black to blackish gray (AD10, AD11). Those in small depressions are aphyric and porous, while those collected from the slope base are fine grained and compact with none or minute phenocrysts of plagioclase.

Excluding AD10 from the western side of the slope base, samples from the depression contain quartz veinlets. Quartz fragments of around 10mm were collected in AD11. Chloritization is advanced in samples AD12 from a small depression and in CB15 from the lower slope.

b. Limestone

Foraminiferal limestone and reefal limestone were collected from all sites.
Foraminiferal limestone is white, pelitic, and soft. Some contain basalt and tuff fragments.

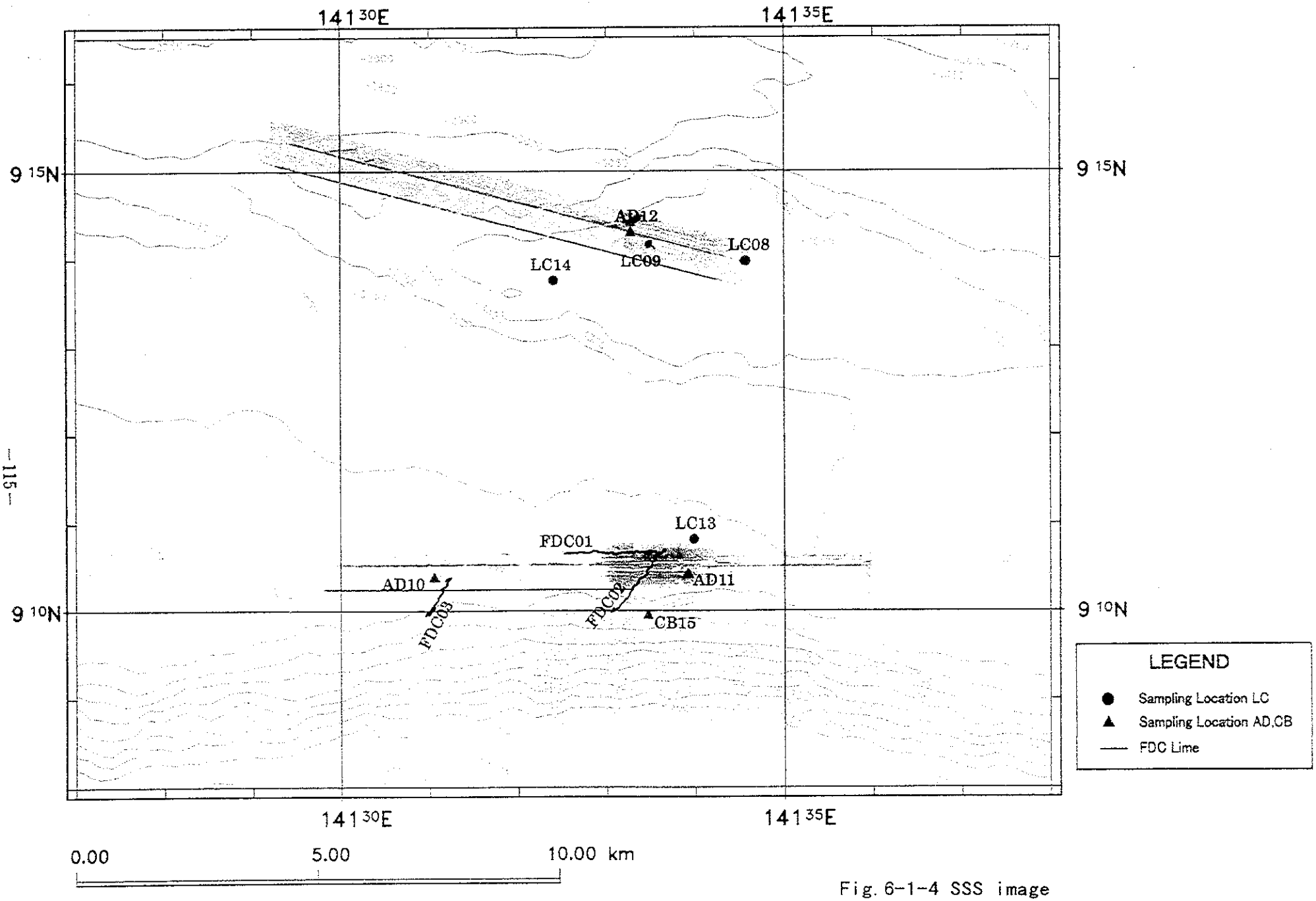

Fig. 6-1-4 SSS image

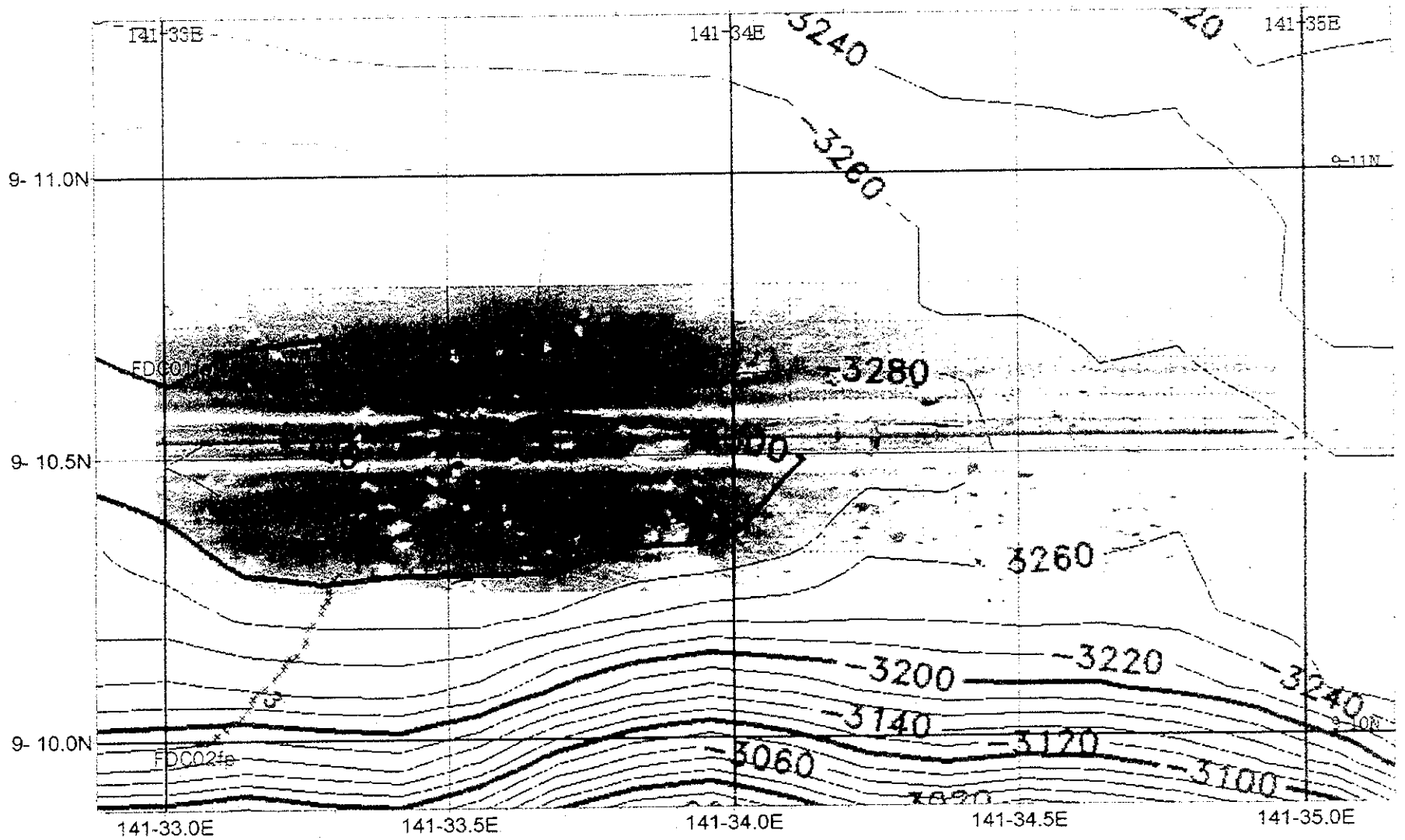

1,2,3,4 are Number of Potographs in FIG.6-2-1.

Fig.6-2-1(1) Location map of seafloor photographs by FDC

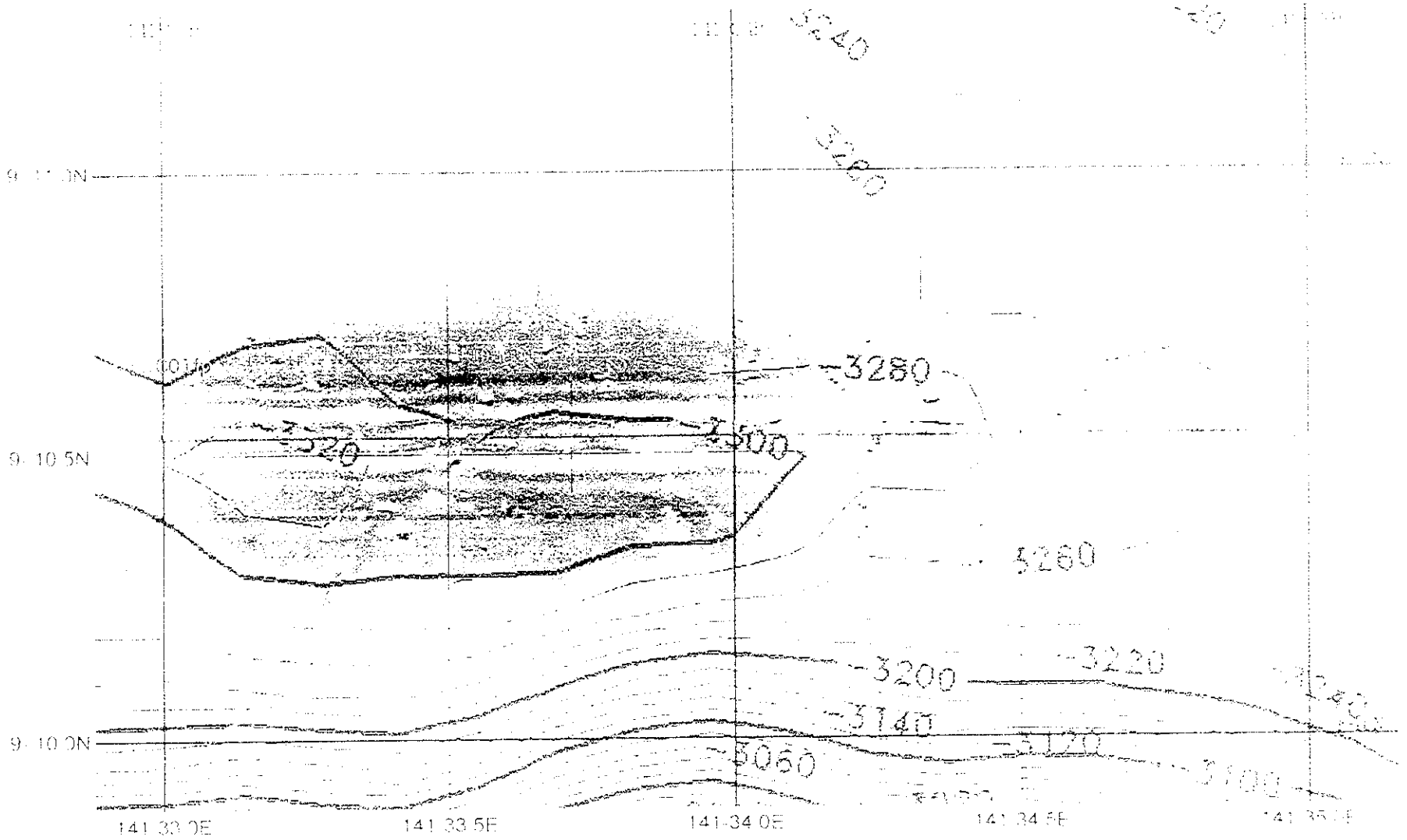

Fig.6-2-1(1) Location map of seafloor photographs by FDC

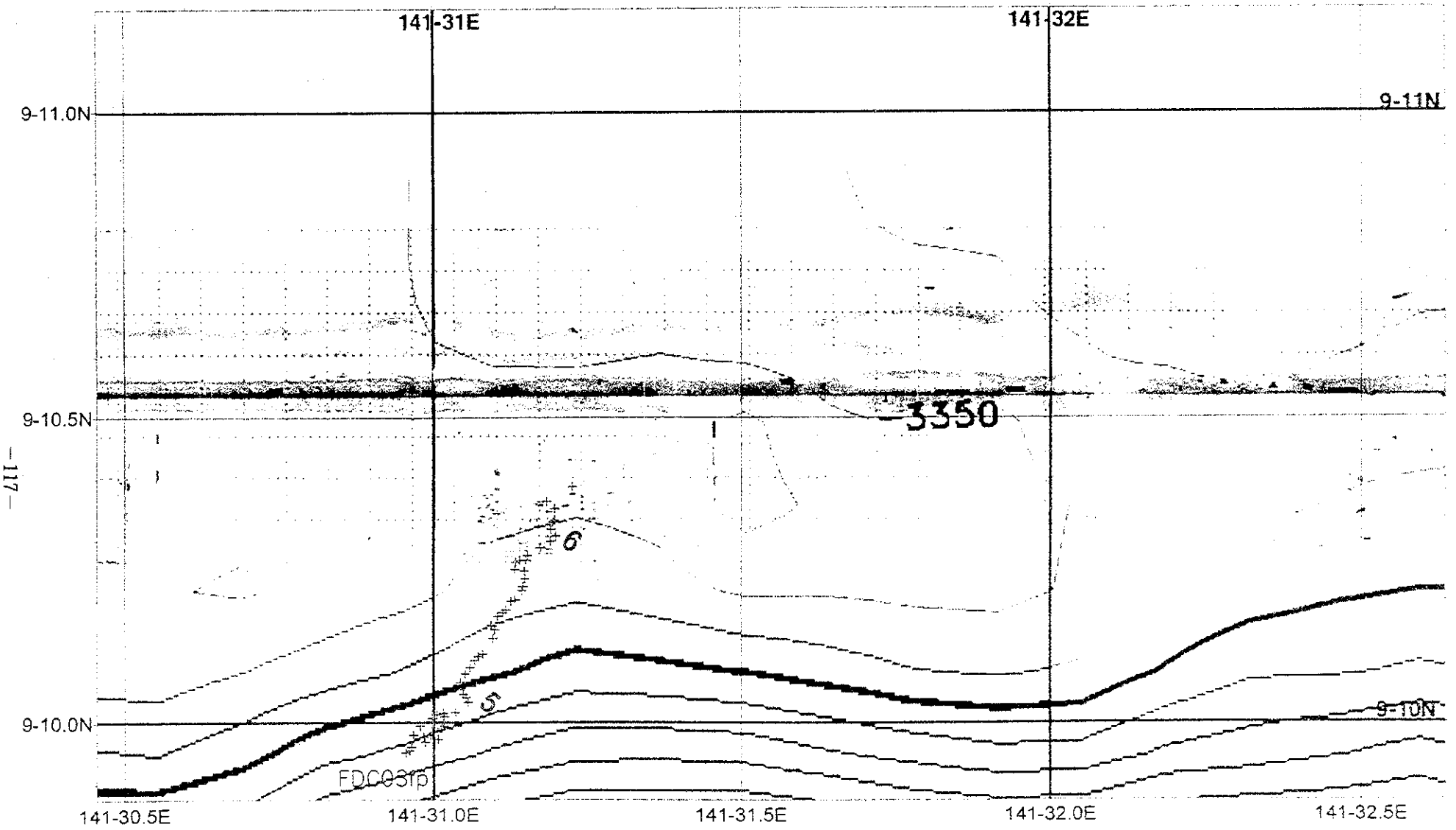

5,6 are Number of Potographs in FIG.6-2-1

Fig.6-2-1(2) Location map of seafloor photographs by FDC

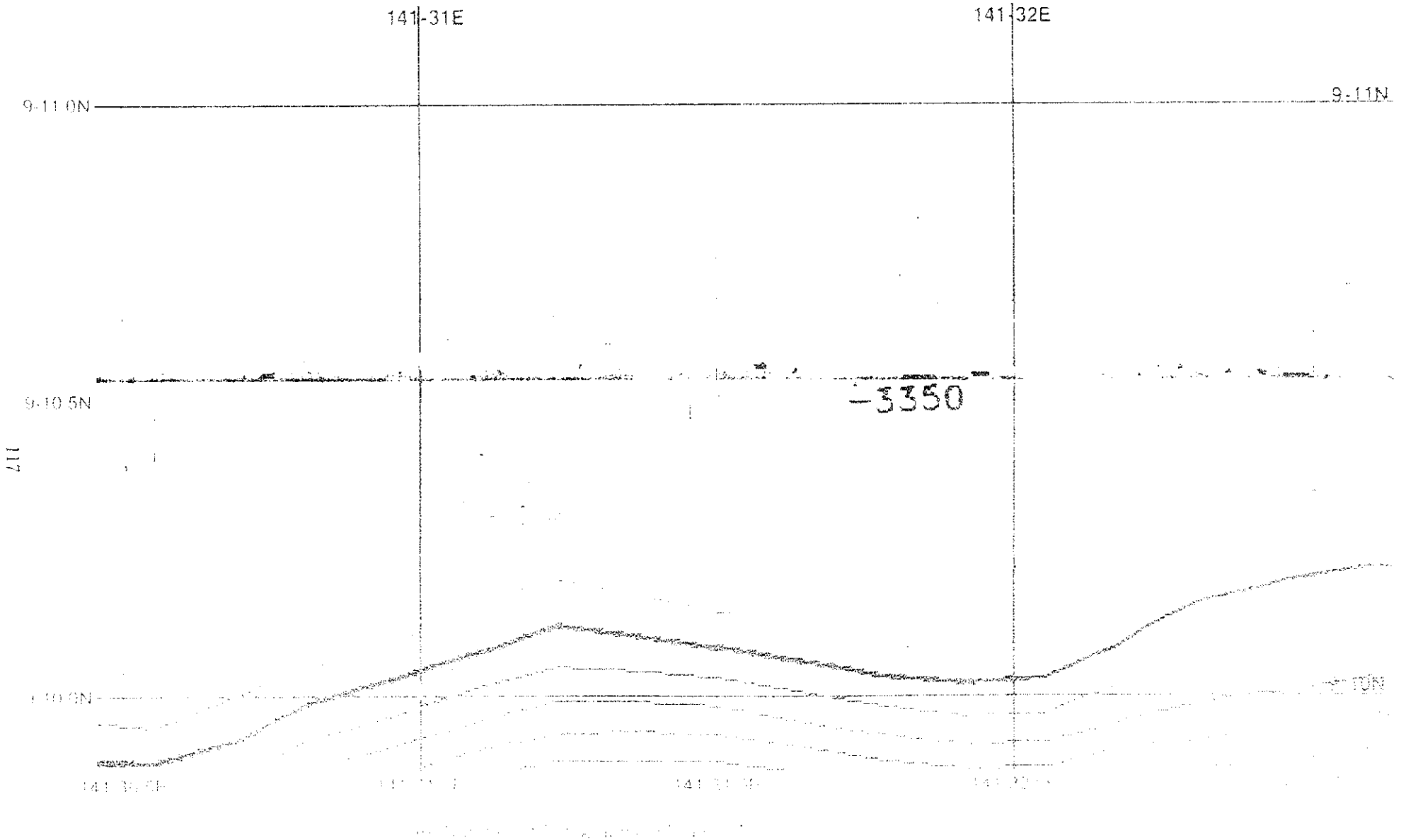

Fig.6-2-1(2) Location map of seafloor photographs by FDC

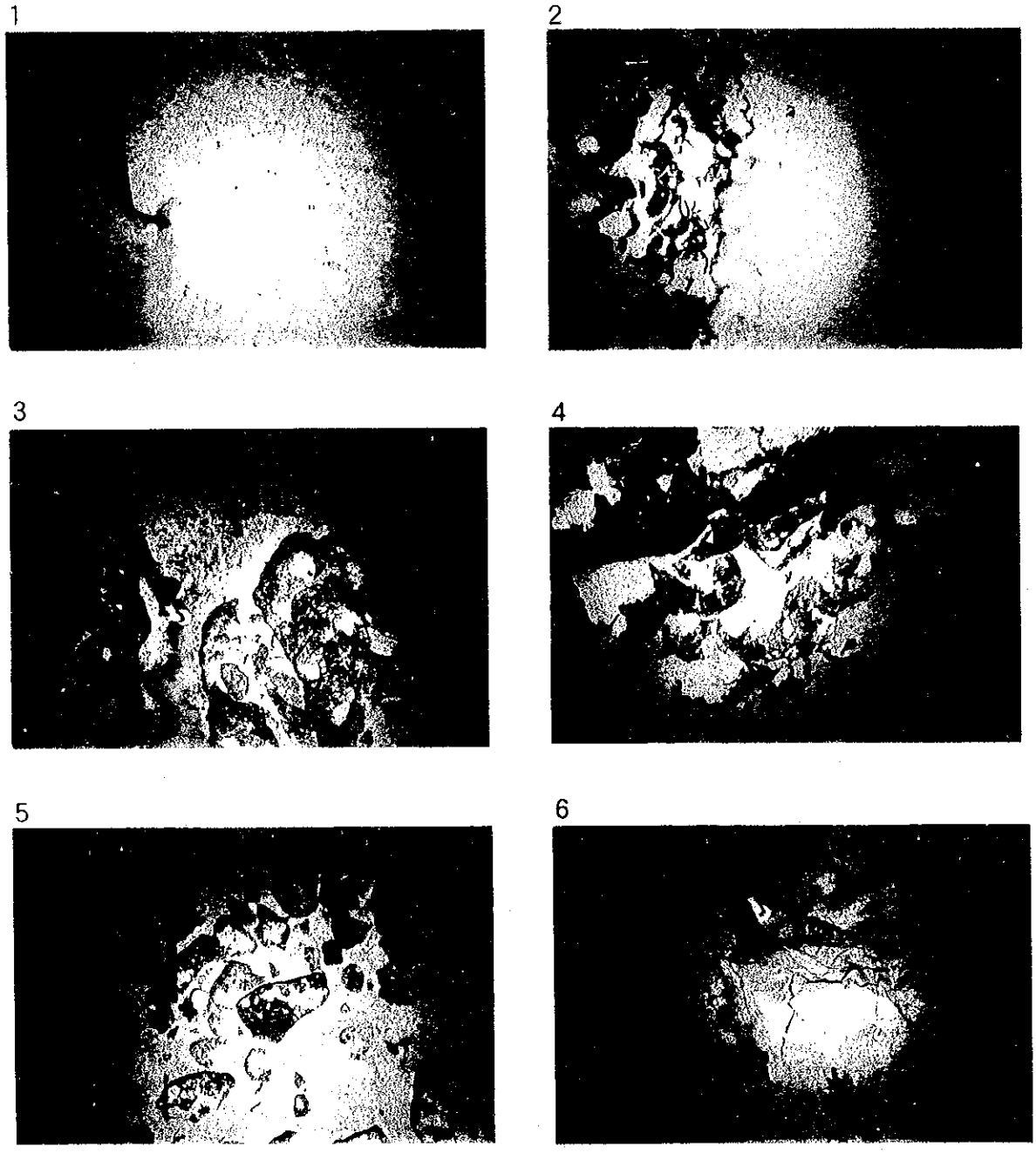

1. 98SMC02FDC01 Foraminiferal sand
   Lower slope Water depth 3,294m 09° 10.676'N 141° 33.419'E
2. 98SMC02FDC01 Crust and foraminiferal sand
   Lower slope Water depth 3,279m 09° 10.680'N 141° 33.560'E
3. 98SMC02FDC02 Crusts
   Lower slope Water depth 3,204m 09° 10.073'N 141° 33.156'E
4. 98SMC02FDC02 Crust on a cliff
   Lower slope Water depth 3,273m 09° 10.517'N 141° 33.500'E
5. 98SMC02FDC03 Talus gravels
   Lower slope Water depth 3,184m 09° 10.049'N 141° 31.068'E
6. 98SMC02FDC03 Limestone
   Lower slope Water depth 3,313m 09° 10.309'N 141° 31.198'E

Fig. 6-2-2 Photographs of FDC seafloor observation

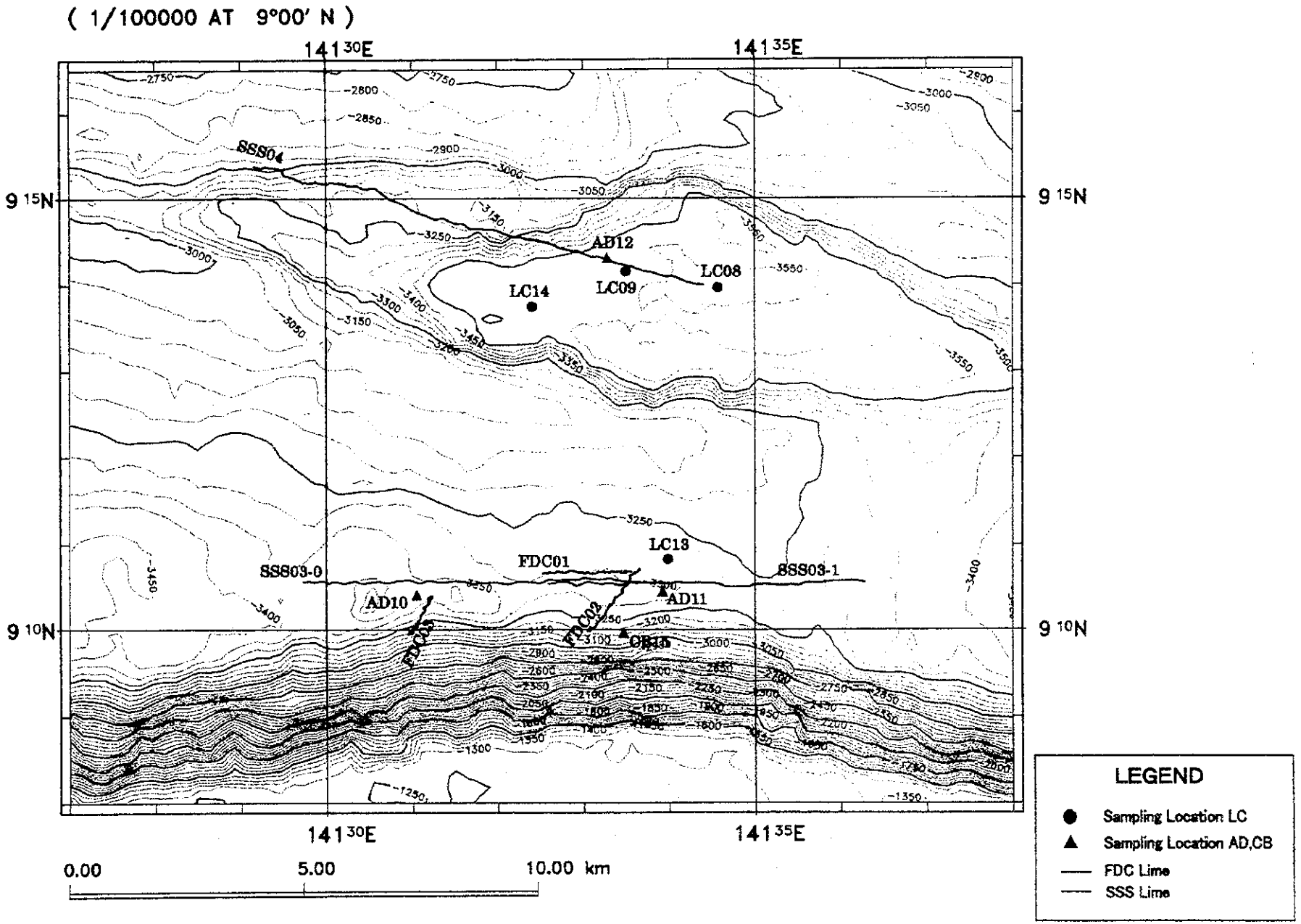

Fig.6-2-3 Location map of sampling sites(MC02 area)

Reefal limestone is milky gray, hard, and some contain coral fragments. Those collected at small depression AD12, and at the lower slope CB15 contain greenish altered parts.

c. Tuffaceous rocks

Tuff samples were collected at three localities aside from CB15 in the lower slope.

They are all well-rounded pebbles, and the matrix is strongly argillized by weathering. They are generally pale green to yellowish green by alteration. The sample from the base of the eastern slope, AD11, is particularly strongly altered and is green.

d. Others

Other than above, 20mm pebble zeolite and 30mm pebble volcanic glass were collected in CB11.

2) Unconsolidated sediments

The four LC sampling was carried out at; one at the foot of a mound from the slope base to the small depression, the other three in the small depression within the bottom of the depression. The columnar sections of the cores recovered by LC are shown in Figure 6-2-5. The stratigraphy is based on that of LC08 and LC14 in the small depression. Both LC08 (328cm long) and LC14 (262cm long) have upper half consisting mainly of brownish gray calcareous clay with intercalations of 1~several millimeters thick magnetite layers. The boundary between the upper and lower half is pale grayish red~pale grayish brown calcareous clay. The lower half of the two cores consists of alternation of blackish brown diatomaceous earth and calcareous clay. Diatomaceous earth occurs near 120cm, and 180cm of LC08 and at 85cm and 110cm of LC14. Near the bottom of these cores; LC09 reached the bedrock in the small depression where sulfur odor was noted, and LC13 which reached the gentle mound has upper half consisting mostly of calcareous clay.

Thin magnetite layers occur in all cores. They are acicular under 1mm in length and often contain fresh foraminifera nucleus, chert fragments, subrounded mudstone pebbles.

(4)Results of laboratory tests

<Rocks>

・ Thin section microscopy and chemical analysis of basalt

Relatively fresh basalt samples from lower northern slope were studied by thin section microscopy and chemically analysed. This is a basalt with micro-phenocrysts of plagioclase and matrix consisting mainly of volcanic glass with minor amount of plagioclase and clinopyroxene. The volcanic glass is partly smectitized but the alteration is weak.

Normative quartz appeared by norm calculation and the rock is classified as tholeiite (Fig. 4-4-1). AFM diagram shows poor MgO content and the rock is plotted in intermediate area between tholeiite and calc-alkaline basalt. Spider diagrams of HFS and LIL elements (Fig. 4-4-2) and of REE (Fig. 4- 4-4) indicate the rock to be P-MORB. It was also plotted in MORB areas of; TiO_2-MnO-P_2O_5 diagram (Fig. 4-4-5), Ti-V diagram (Fig. 4-4-6), and Zn-Nb-Y diagram (Fig. 4-4-7). From the above this basalt is classified as P-MORB. Together with the results of the previous survey, it is clarified that P type-MORB is

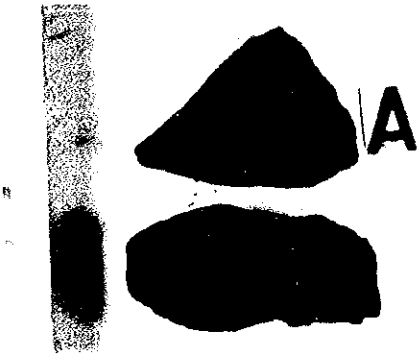

Open Nicol

A. 98SMC02AD11-A
Microphyric basalt
Yellow greenish brown colored.
Alteration hardly appearing.

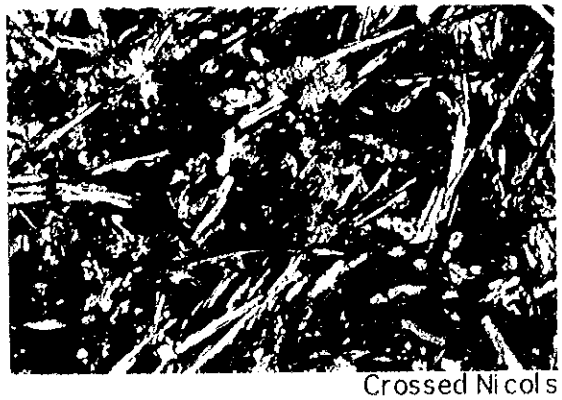

Crossed Nicols

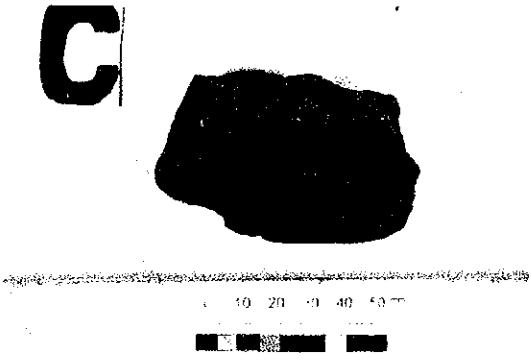

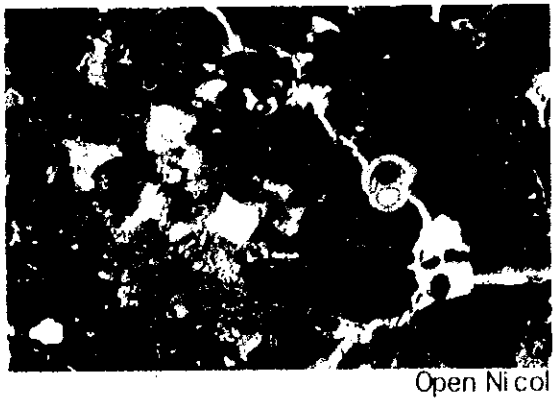

Open Nicol

B. 98SMC02AD11-C
Mudstone
Tufficious. Yellow greenish colored.
Including foraminifera fossils.

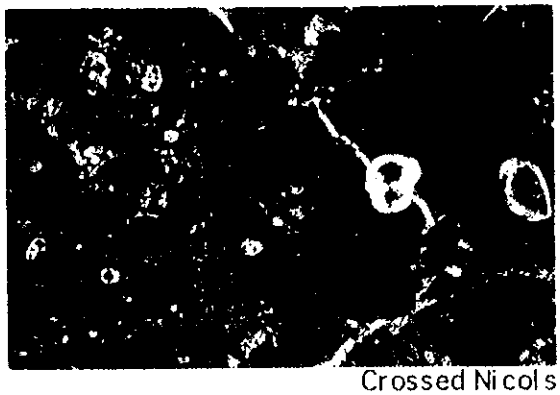

Crossed Nicols

Fig 6-2-4(1) Photographs of rocks sampled at MC02 area.

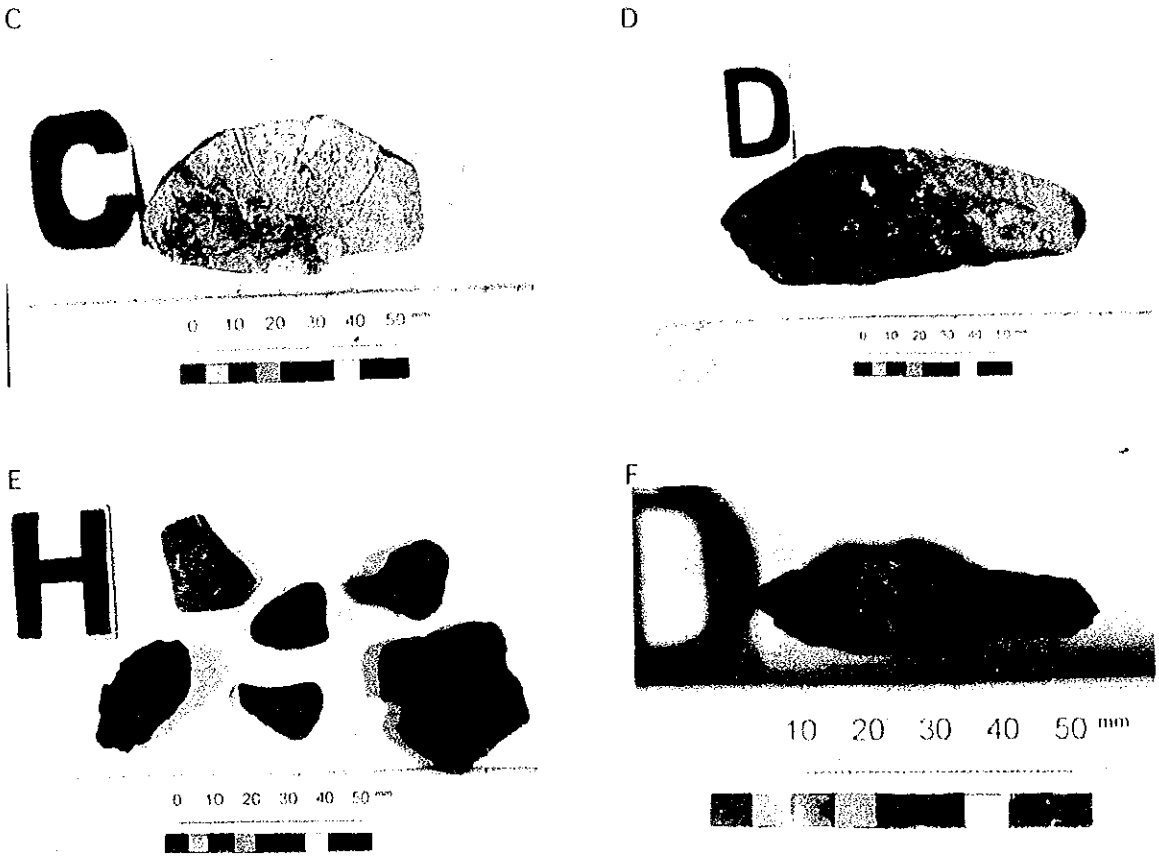

C. 98SMC02AD10-C
Foraminifera carbonate limestone
Including rubbles a little.
D. 98SMC02AD12-D
Foraminifera carbonate limestone
Dyed with manganese oxide.
E. 98SMC02AD11-H
Tuff
Altered propylitization a little.
F. 98SMC02AD11-D
Basalt with quartz vein.

Fig 6-2-4(2) Photographs of rocks sampled at MC02 area.

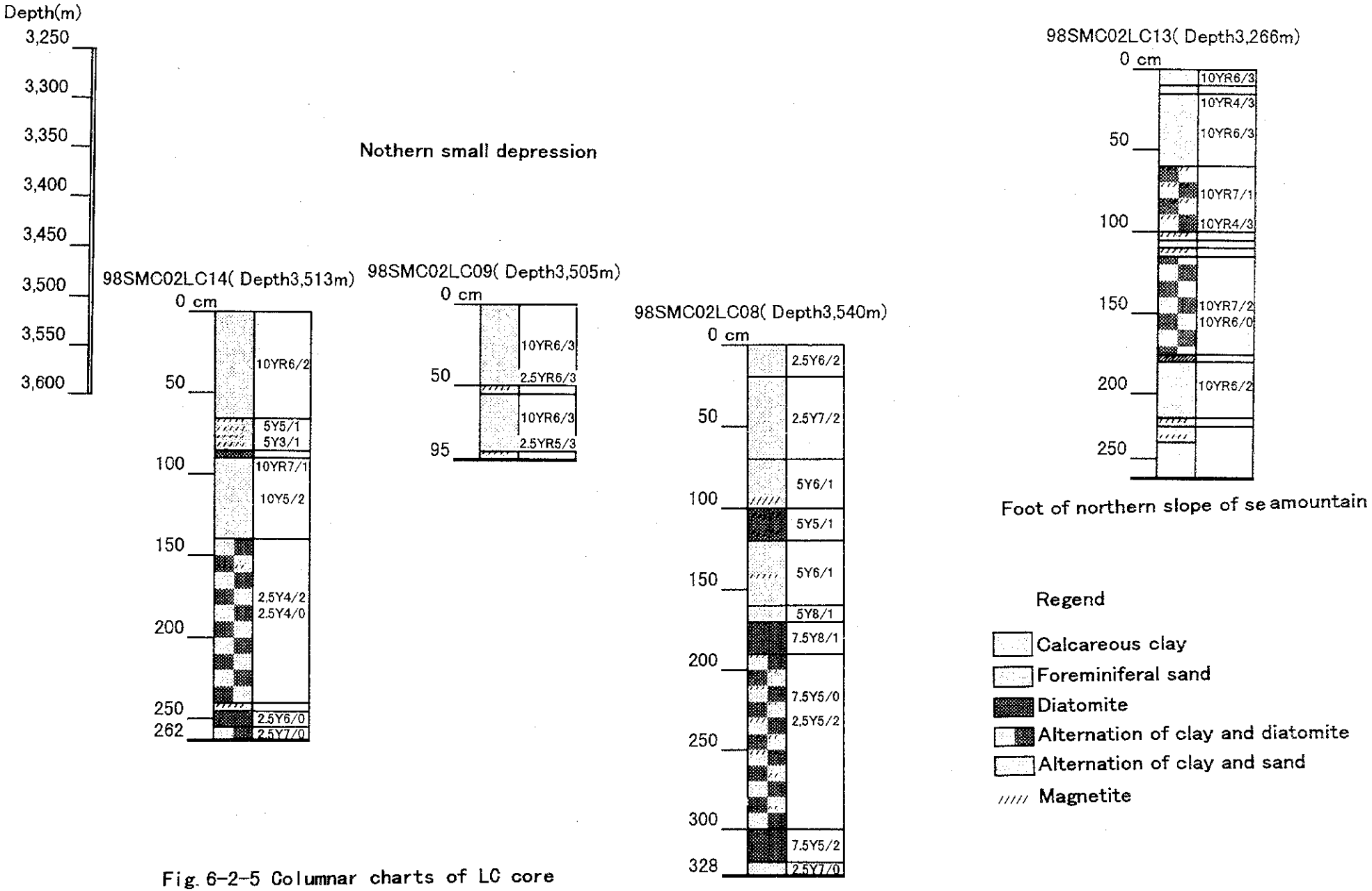

Fig. 6-2-5 Columnar charts of LC core

distributed on the seamount slope of the MC02 area, and this fact indicates that there were igneous or volcanic activities which resulted in formation of P-MORB.

・The result of observation of microfossile in limestone

The observation of microfossile in limestone which are sampled in the foot of the northern slope, is carrie out.Some planktonic foraminiferal fossil of Oligocene could be found but it is impossible to determine the geological age. The benthonic foraminiferal fossil are shown ages of Eocene ~ Oligocene so it is also impossible to determine the geological age. The benthonic foreminiferal fosshil are including many speaces of long term, ant it means that this lime stone has origin of secondaly sediment as turbidite.

・X-ray diffraction and thin section microscopy of altered rocks

Strongly altered basalt, tuff, and mudstone containing fine-grained minerals were dredged from the slope. X-ray diffraction was carried out on basalt and tuff samples. Sulfide minerals such as pyrite were not identified, but propylitization, a type of hydrothermal alteration, was confirmed. Mudstone samples were studied by thin section microscopy. It was confirmed that the fine-grained minerals were volcanic glass, quartz and basalt fragments, sulfide minerals were not observed.

<Bottom sediments>

X-ray diffraction and microfossil identification were carried out on cores by LC from a small depression on the northern side. The samples used were LC14 sampling core. The sampling depth and observation by unaided eyes are shown in Table 6-2-1.

Table 6-2-1 Analyzed Samples

Sample	Collected depth	Description
Fm04	76-81cm	Homogeneous milky white fine sand. Contain many black to brown sand.
Fm07	107-108cm	Yellowish very fine sand. Contain black to brown sand.
X03	121cm	Homogeneous milky white silt. Contain small amount of mafic minerals.
Fm14	251-252cm	Light gray fine sand.

The brown to black sand grains in samples Fm04, Fm07, and X03 are magnetite with relatively clear acicular form by unaided eyes.

・Results of X-ray diffractometry

Strong calcite peaks are detected from all samples. This is caused by identifying foraminifera as calcite. Chlorite/montmorillonite mixed-layer minerals and sericite/montmorillonite mixed-layer minerals occur in all samples. These are hydrothermal alteration minerals, but these occur in minute amount and other alteration minerals are not observed, and these are believed to have been formed elsewhere and transported by wind or other media. Sulfide minerals were not identified.

・Results of microfossil identification

The results of microfossil identification are laid out in Table 6-2-2, photographs of typical foraminifera and radiolaria are shown in Figures 6-2-6 and 6-2-7 (1),(2).

Table 6-2-2 Results of fossil observation of seafloor sediment

Area	Sampling No.	Sample No.	Sampling Depth(m)	Sample	Foraminifera		Geological age	Absolute age (Ma)	Radiolaria	Geological age	Absolute age (Ma)
					Planktonic	Benthonic					
MC02	LC14	Fm04	1,506	Fine sand	many	rare	Pliocene	5.6-3.12	few	After late Pliocene	2.78-
		Fm07	1,325	Very fine sand	many	rare	Pleistocene	2.0-	A little many	After middle Pliocene	3.5-
		X03	1,468	Silt	many	rare	Pliocene	5.6-3.12	A little many	After late Pleistocene	0.18-
		Fm14	2,284	Fine sand	many	few	Pliocene	5.6-3.12	A little few	After middle Pliocene	3.5-

From the results of identification of foraminifera and radiolaria, it is concluded that the four samples studied are all redeposited material. Regarding foraminifera, early Pliocene ~ early-late Pleistocene and Miocene species occurred in all samples; and as for radiolaria, late Paleocene ~ early Miocene and late-middle Miocene species were confirmed in all samples.

Since Pleistocene foraminifera occur in Fm07 and late Pleistocene ~ Holocene, radiolaria occur in X03, sediments in stratigraphically higher position than X03 are believed to have deposited after late Pleistocene. On the other hand, Fm14 is believed to have deposited after middle Miocene from the age of radiolaria fossils. Also Fm14 contain; large foraminifera, very few foraminifera fragments, and no Pleistocene individuals; indicating depositional environment different from that of sediments stratigraphically higher than X03.

The distribution of radiolaria fossils in sediments higher than X03 indicate that these fossils were stirred, transported, and redeposited by intermittent bottom currents flowing at several centimeters per second.

From the above, it is considered that in this depositional site during late Pleistocene - Holocene time, there were weak bottom currents capable of stirring and transporting 200 μ m radiolaria fossils from upper Paleocene - lower Miocene Series

Surface sediments which contain large amount of redeposited radiolaria fossils from upper Paleocene - lower Miocene Series are distributed widely from the central to the western part of the Equatorial Pacific (Dinkelman, 1973; Johnson and Parker, 1972; Moore, 1995; Riedel, 1954, 1957; Riedel and Funnell, 1964). The core studied in the present project is from the above sea area. The supply process of the redeposited radiolaria is explained by Johnson and Parker (1972) as the result of denudation and redeposition due to stronger circulation of the surface・deep current during the Pleistocene glacial age. In the present case, this explanation does not apply, because the strata containing redeposited-radiolaria occur regardless of the glacial or interglacial period.

6-3 Temperature Gradient

Thermister was attached to LC and the temperature gradient of the sediments were measured. The results are shown in Figure 6-3-1.

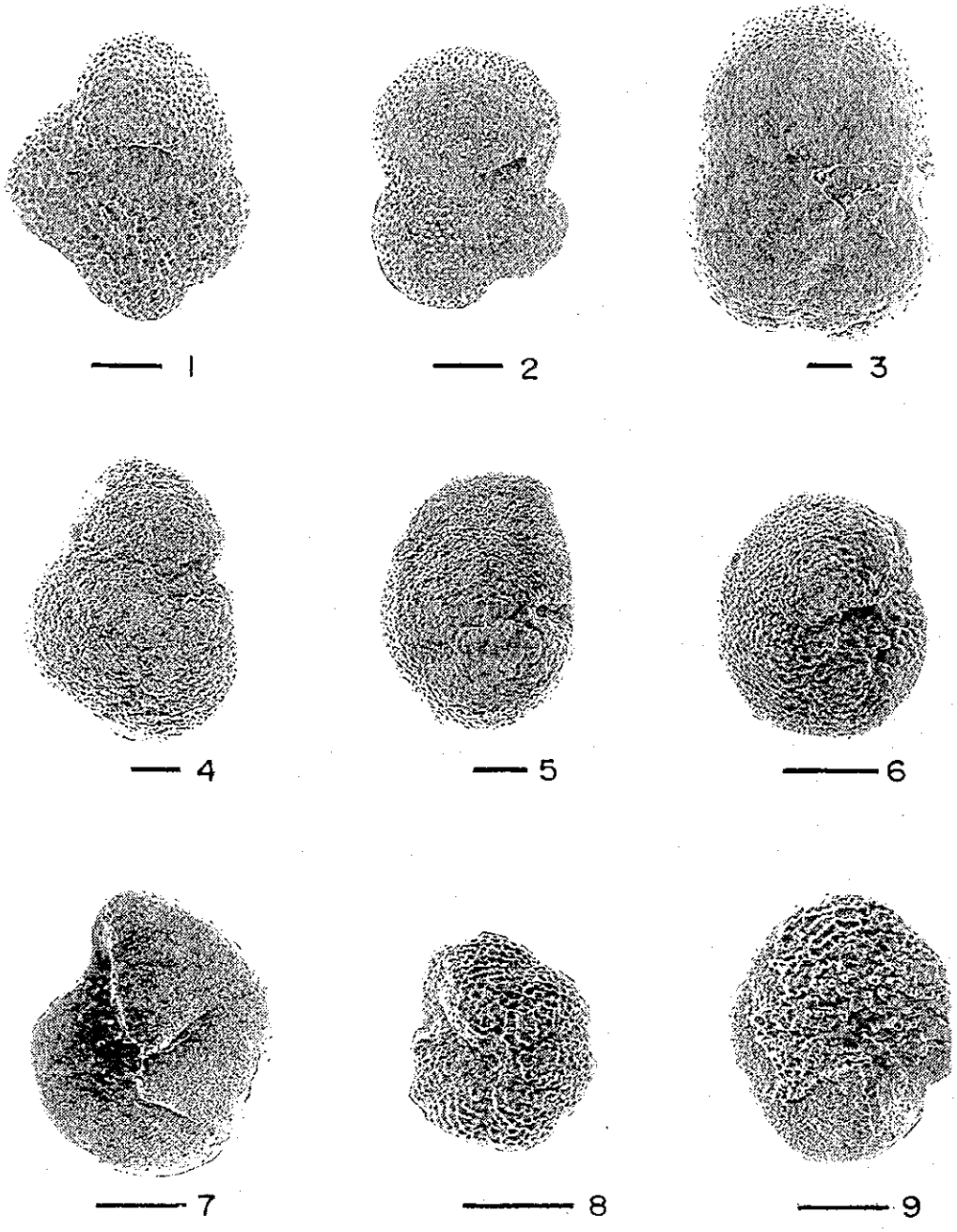

Scale bars: 100 μ m

1. Globigerinoides obliquus extremus (Bolli). Umbilical view, Sample from 98SMC02LC14Fm07.
2. Globigerinita glutinata (Egger). Umbilical view, Sample from 98SMC02LC14Fm07.
3. Sphaeroidinella dehiscens (Parker and Jones). Umbilical view, Sample from 98SMC02LC14Fm14.
4. Sphaeroidinellopsis seminulina (Schwager). Umbilical view, Sample from 98SMC02LC14Fm04.
5. Globorotalia tumida (Brady). Umbilical view, Sample from 98SMC02LC14Fm14.
6. Globorotalia tosaensis Takayanagi and Saito. Umbilical view, Sample from 98SMC02LC14Fm07.
7. Globorotalia truncatulinoides (d'Orbigny). Umbilical view, Sample from 98SMC02LC14Fm07.
8. Globorotalia kugleri Bolli. Umbilical view, Sample from 98SMC02LC14Fm04.
9. Globorotalia peripheroronda Blow and Banner. Umbilical view, Sample from 98SMC02LC14Fm04.

Fig. 6-2-6 Species of the Typical Foraminifera Fossils

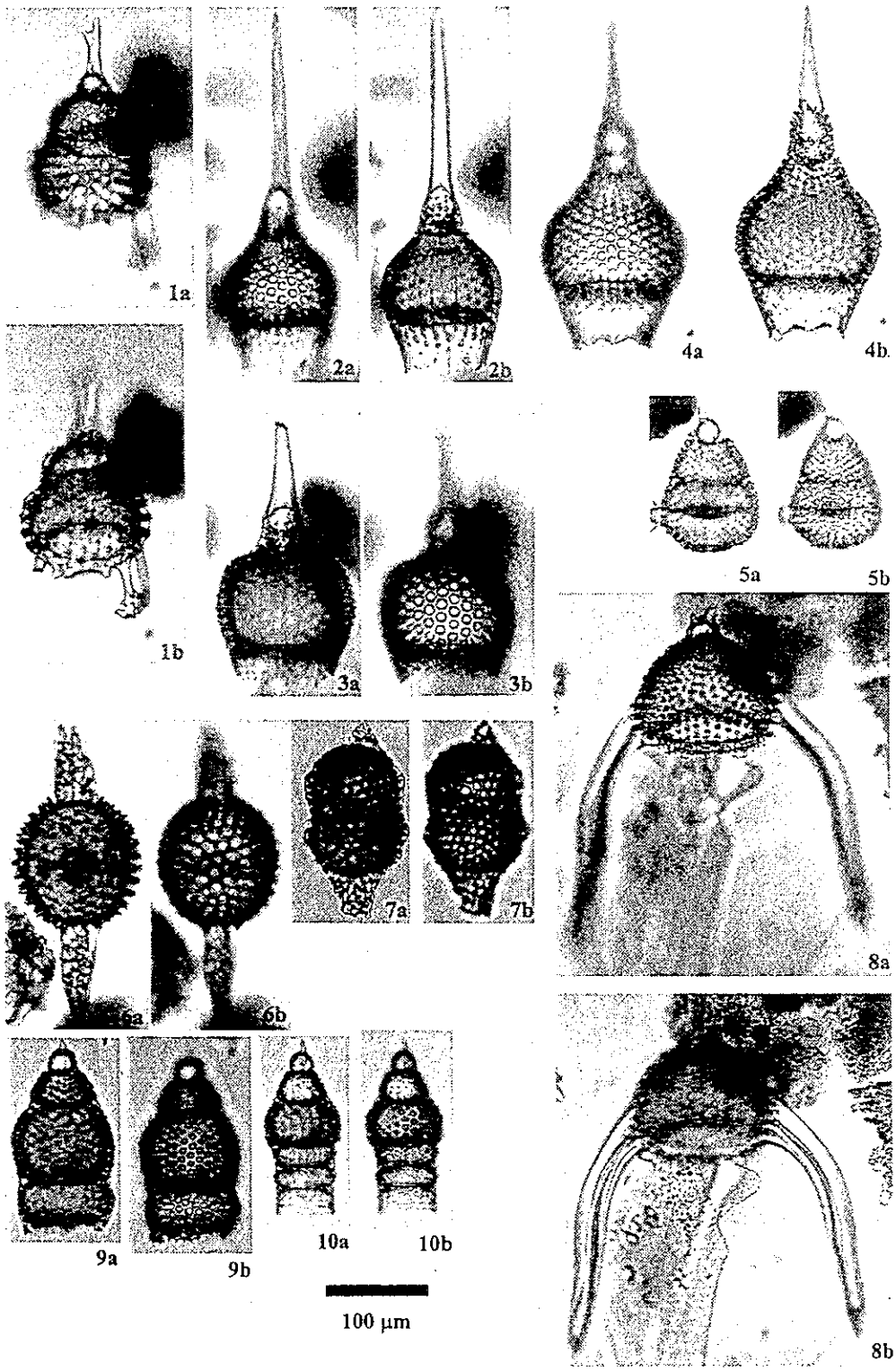

1a-b. *Artophormis gracilis* Riedel
Photo ID: 03033, 03034 (LC14X03)

2a-b. *Calocycletta costata* (Riedel)
Photo ID: 03078, 03079 (LC14X03)

3a-b. *Calocycletta robusta* Moore
Photo ID: 03091, 03092 (LC14X03)

4a-b. *Calocycletta serrata* Moore
Photo ID: fm04-011, fm04-012 (LC14fm04)

5a-b. *Cyrtocapsella tetrapera* Haeckel
Photo ID: 03095, 03096 (LC14X03)

6a-b. *Didymocyrtis prismatica* (Haeckel)
Photo ID: 03130, 03131 (LC14X03)

7a-b. *Didymocyrtis mammifera* (Haeckel)
Photo ID: fm07-023, fm04-024 (LC14fm04)

8a-b. *Lychnocanoma elongata* (Vinassa)
Photo ID: fm04-009, fm04-010 (LC14fm04)

9a-b. *Stichocorys delmontensis* (Campbell and Clark)
Photo ID: 03116, 03117 (LC14X03)

10a-b. *Stichocorys wolffii* Haeckel
Photo ID: 03121, 03122 (LC14X03)

Fig. 6-2-7(1) Species of the Typical Radiolarian Fossils

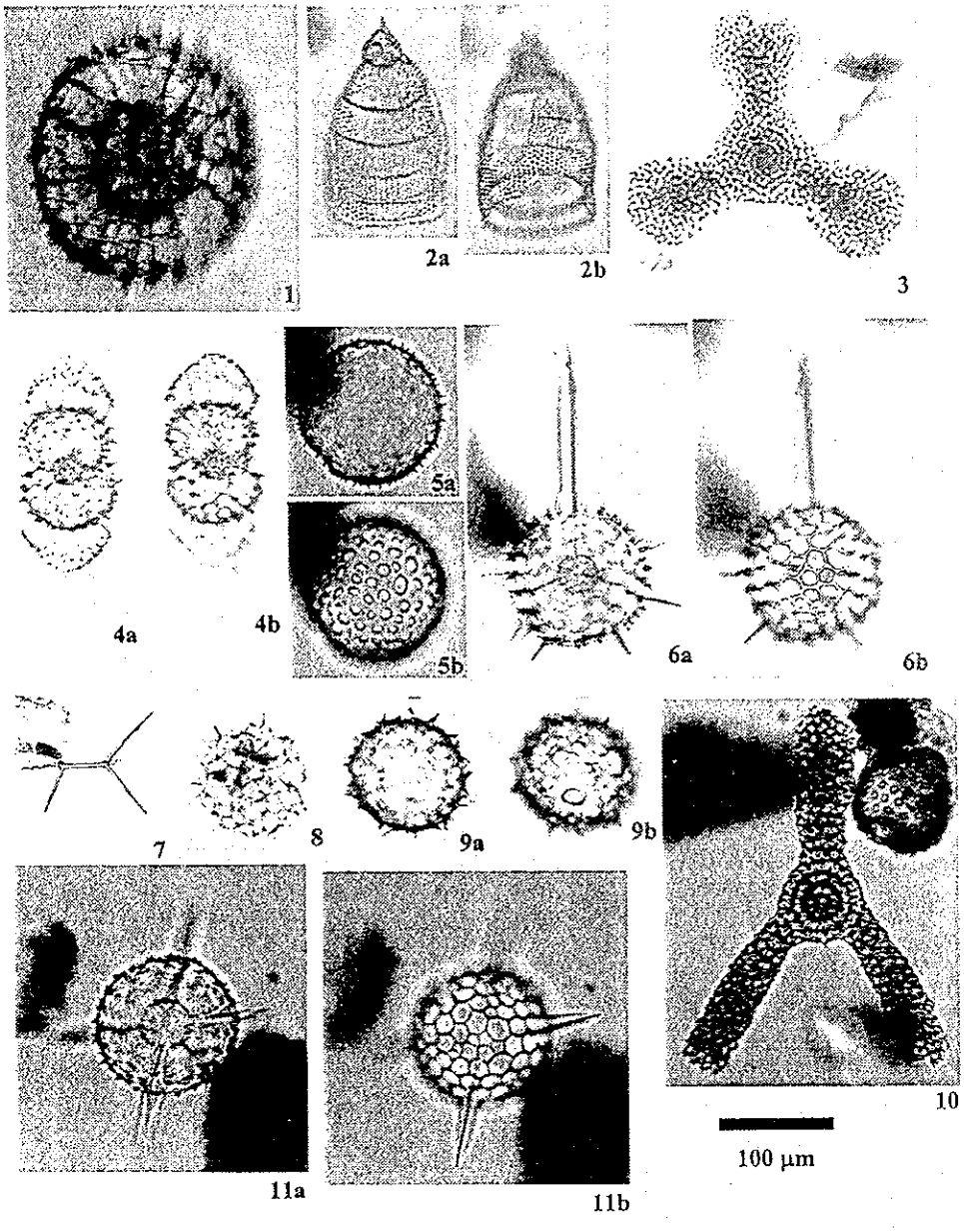

1. *Spongoplegma medianum* (Nigrini)
Photo ID: fm07-030 (LC14fm07-030)

2a-b. *Eucyrtidium hexagonatum* Haeckel
Photo ID: 03089, 03090 (LC14X03)

3.*Euchitonia zitteli* (Stohr)
Photo ID: 03030 (LC14X03)

4a-b. *Didymocyrtis tetrathalamus tetrathalamus* (Haeckel)
Photo ID: 03035, 03036 (LC14X03)

5a-b. *Siphonosphaera cyathina* Haeckel
Photo ID: 03109, 03110 (LC14X03)

6a-b. *Carpocanthum monostylus* (Caultet)
Photo ID: 03005, 03006 (LC14X03)

7. *Sphaerozoum* sp.
Photo ID: 03025 (LC14X03)

8. *Spongoplegma* sp.
Photo ID: 03026 (LC14X03)

9a-b. *Acrospahera spinosa* (Haeckel)
Photo ID: 03007, 03008 (LC14X03)

10. *Euchitonia mulleri* Haeckel
Photo ID: 03088 (LC14X03)

11a-b. *Hexacontium* spp.
Photo ID: 03073, 03074 (LC14X03)

Fig. 6-2-7(2) Species of the Typical Radiolarian Fossils

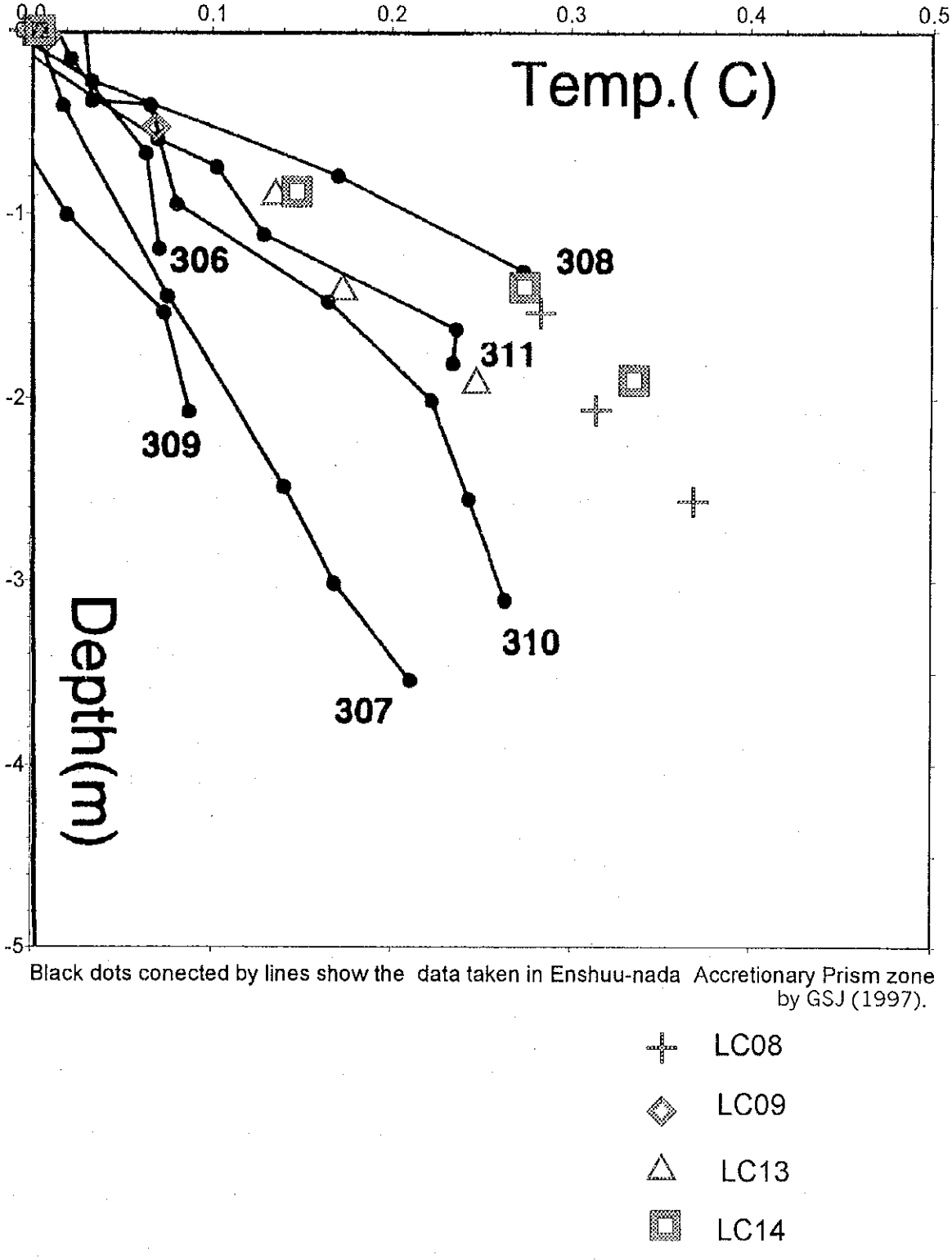

Fig.6-3-1 Geothermal gradient

Similar temperature gradient is obtained at all points. The small difference would be that the gradient of LC13 near the base of the slope is low, while that of LC08 and LC14 in the small depression is high. In the figure, the results of data acquired by similar method by the Geological Survey of Japan (GSJ) accretionary belt which continues to the Nankai Trough are also shown. It is seen from the above that the heat flow in the MC02 depression is in the same order as in low temperature water flow area of accretionary belts.

6-4 Discussions (on hydrothermal activities)

The results of the present survey in MC02 area where the possibility of hydrothermal activities were indicated by acquisition of pyrite-disseminated basalt samples during the 1997 survey.
Figure 6-3-1.

1. The depression on the northern side is wholly covered by unconsolidated sediments. The sediments are 10~20m thick from the base of the seamount to near 9° 15'N, but the thickness tends to increase reflecting the valley-type basement structure.
2. Coarse sands and pebbles are distributed partly as unconsolidated sediments covering the seafloor to the south of 9° 15'N.
3. The small depression on the northern side is wholly covered by sediments, but there are localities with thin sedimentary cover suggesting the rise of the basement. Also mound-type rises are observed on the seafloor between the small depression to the steep slope base. These mounds are believed to be pillow lava covered by foraminiferal sand.
4. The basalt constituting the steep slope on the northern side of the seamount is classified as P-MORB from chemical analysis. It is inferred from the data acquired by the 1997 and the present surveys that there were, in this area, volcanic and hydrothermal activities which formed this P-MORB in early Miocene.
5. It was observed that angular pebbles are deposited on the base of the steep slope where pyrite-disseminated basalt was collected in 1997. Disseminated samples were not dredged this year at the base, but propylitized basalt and tuff samples were collected.
6. Sulfur odor was in from the unconsolidated sediments from the depression. Although sulfides and alteration products were not found, several sand layers containing magnetite were confirmed. The magnetite crystals are idiomorphic with clear edges, not transported, and is believed to have been formed in the small depression.
7. From the results of radiolaria fossil identification, the small depression is believed to have been under intermittent sea water flow since Pleistocene. Sediments were stirred by this water flow, and there could have been spring water flowing out from the bottom of the small depression.
8. The heat flow of the MC02 area is inferred to be similar to the low-temperature water flow zone of the accretionary belt, from the results of temperature gradient measurement of the sediments.

The geologic history of the MC02 area is inferred as follows from the above survey results.

Dolerite was formed on the northern steep slope by volcanic activity in early Miocene. The volcanic activity continued, and the rise of the basement of the small depression in the trench topography is believed to be the result of intrusion of basalt associated with spreading of the depression. Also the pillow lava mounds between the slope base and the small depression are considered to be associated with the basalt

intrusion into the small depression. Hydrothermal solution associated with the volcanism rose through the fault plane which corresponds to the present northern steep slope and the basalt was disseminated.The hydrothermal activity continued and rise of hydrothermal solution occurred in the small depression during Pleistocene.

From the above discussions, it is possible that hydrothermal deposits occur at the base of the steep slope where pyrite dissemination was confirmed and also in the small depression where evidence of hydrothermal activity has been observed. On the steep slope, however, angular pebbles are deposited and the ore is believed to occur under the pebbles or mixed with them.

Neither sulfides nor alteration minerals were collected from the small depression during the present survey. But magnetite which is believed to have been formed in the small depression have been confirmed in the sediments, and there is a possibility of hydrothermal deposit formation below the sediments.